Simulation of Electron-Proton Coupling with a Monte Carlo Method: Application to Cytochrome c_3 Using Continuum Electrostatics

António M. Baptista, Paulo J. Martel, and Cláudio M. Soares
Instituto de Tecnologia Química e Biológica, Universidade Nova de Lisboa, 2781-901 Oeiras, Portugal

ABSTRACT A new method is presented for simulating the simultaneous binding equilibrium of electrons and protons on protein molecules, which makes it possible to study the full equilibrium thermodynamics of redox and protonation processes, including electron-proton coupling. The simulations using this method reflect directly the pH and electrostatic potential of the environment, thus providing a much closer and realistic connection with experimental parameters than do usual methods. By ignoring the full binding equilibrium, calculations usually overlook the twofold effect that binding fluctuations have on the behavior of redox proteins: first, they affect the energy of the system by creating partially occupied sites; second, they affect its entropy by introducing an additional empty/occupied site disorder (here named *occupational entropy*). The proposed method is applied to cytochrome c_3 of *Desulfovibrio vulgaris* Hildenborough to study its redox properties and electron-proton coupling (redox-Bohr effect), using a continuum electrostatic method based on the linear Poisson-Boltzmann equation. Unlike previous studies using other methods, the full reduction order of the four hemes at physiological pH is successfully predicted. The sites more strongly involved in the redox-Bohr effect are identified by analysis of their titration curves/surfaces and the shifts of their midpoint redox potentials and pK_a values. Site-site couplings are analyzed using statistical correlations, a method much more realistic than the usual analysis based on direct interactions. The site found to be more strongly involved in the redox-Bohr effect is propionate D of heme I, in agreement with previous studies; other likely candidates are His^{67}, the N-terminus, and propionate D of heme IV. Even though the present study is limited to equilibrium conditions, the possible role of binding fluctuations in the concerted transfer of protons and electrons under nonequilibrium conditions is also discussed. The occupational entropy contributions to midpoint redox potentials and pK_a values are computed and shown to be significant.

INTRODUCTION

Redox processes are among the key functional aspects of living organisms, being involved in such important phenomena as respiration and photosynthesis. Many factors can affect or modulate redox processes, one of the more important being the pH of the medium: redox proteins often show a strong dependence of midpoint redox potentials (E^{half}) on pH and a corresponding dependence of midpoint pK_a values (pK^{half}) on potential, a phenomenon known as the redox-Bohr effect (Papa et al., 1979; Xavier, 1985). Given the fundamental electrostatic nature of the two types of processes, the existence of such a dependence is hardly surprising; instead, it would be strange if no coupling were found, considering the strength and long-range character of electrostatic interactions. Despite this nonspecific chemical-physical origin of the redox-Bohr effect, it is likely that evolution has "explored" this aspect and developed more specific and functionally relevant electron-proton couplings, which are thus expected to be present in many redox proteins.

The study of biomolecular systems by theoretical computational methods depends, to a great extent, on how closely one manages to model the actual in vivo or in vitro physical conditions of the system being investigated. Even when we limit ourselves to the study of the more easily modeled equilibrium conditions typical of in vitro systems, as is the case here, the nature of the models should be carefully considered. In particular, special attention must be given to the choice of external parameters of the system, the most important of which are the temperature and pressure and, in the case of electron-proton coupling, the electrostatic potential and pH. (In statistical mechanical terms, this corresponds to the choice of a proper ensemble.) Hence, our system of interest is a protein whose protonatable and redox sites display equilibrium fluctuations of state, and not an isolated protein with a particular redox and protonation state. If we regard the protein as "static" from the viewpoint of electron and proton binding, we will obtain a distorted picture of its behavior; in particular, some entropic factors will be lost (see below).

The level of treatment given to the external parameters (temperature, pressure, pH, electrostatic potential) is in general different for each computational method, and a complementary approach using several methodologies may be necessary. There are two major methodological routes to the study of equilibrium biomolecular processes that are essentially electrostatic in nature, such as redox or (de)protonation processes: molecular mechanics (MM) and continuum electrostatic (CE) methods.

Received for publication 14 October 1998 and in final form 24 February 1999.

Address reprint requests to Dr. António M. Baptista, Instituto de Tecnologia Química e Biológica, Universidade Nova de Lisboa, Apartado 127, 2781-901 Oeiras, Portugal. Tel.: 351-1-446-9613; Fax: 351-1-441-1277; E-mail: baptista@itqb.unl.pt.

0006-3495/99/06/2978/21 $2.00

The MM approach treats the protein as a flexible molecule surrounded by moving water molecules, the electrostatic interactions being just one of the various types of interactions between the atoms; conformational changes can then be studied by using molecular dynamics (MD) simulations. Because a single redox and protonation state of the protein has to be used, redox and protonation changes can be studied not with pure MD, but rather by using MM-based free energy methods (Zwanzig, 1954; Mezei and Beveridge, 1986; Beveridge and DiCapua, 1989). MM-based free energy calculations have been used with some success to compute redox potentials (Churg and Warshel, 1986; Cutler et al., 1989; Langen et al., 1992; Mark and van Gunsteren, 1994; Alden et al., 1995; Apostolakis et al., 1996; Muegge et al., 1997; Soares et al., 1998) and pK_a values (Warshel, 1981; Russell and Warshel, 1985; Warshel et al., 1986; Lee et al., 1993; Del Buono et al., 1994) in protein molecules; as usual, calculated values are relative to model compounds or to changes in the protein (mutations). The major problem with MM-based free energy calculations is their high computational cost, which led to the development of approximate methods, usually involving partial rigidification and/or some form of linear response hypothesis (Warshel and Russell, 1984; Muegge et al., 1997; Levy et al., 1991). Nevertheless, when many changes have to be considered simultaneously, such as when treating multiple proton equilibrium (a protein with s protonatable sites has 2^s different states), the MM approach is too demanding (less so if one uses a pairwise approximation; Del Buono et al., 1994) and cannot be used to make a complete study of the simultaneous protonation and redox equilibria in proteins. Although the MD approach can be extended to treat the effect of binding (Baptista et al., 1997), the resulting methods are still too demanding for the type of study we are interested in here.

The CE approach treats the protein and solvent as two distinct dielectric media, the protein atoms being represented as point charges in a static (average) molecular structure; a counterion atmosphere surrounds the protein, and the whole system is described by the Poisson-Boltzmann equation (Sharp and Honig, 1990; Honig and Nicholls, 1995). The free energies associated with charge modifications are then computed as the electrostatic energy change in this two-dielectric model. If the linear form of the Poisson-Boltzmann equation is used, the energy thus obtained is by definition pairwise decomposable. (Although potentials on the counterion region may exceed kT/e, the use of the nonlinear form poses nonadditivity problems that can only be solved by introducing additional approximations (Vorobjev et al., 1994); as usual in CE multiple binding problems, we will assume that the linear form gives reasonable potential values at protein atoms.) Thus, besides its modest computational requirements (compared with MD simulations), this approach directly produces a set of additive free energy contributions that makes it possible to address the simultaneous change of many charge states in a protein molecule. These states have to be weighted by using some additional method, the most general of which is perhaps a Monte Carlo (MC) method (Antosiewicz and Porschke, 1989; Beroza et al., 1991). The most evident problem of the CE approach is the use of a rigid protein structure: either we restrict the method to (hypothetical) rigid molecules (Baptista et al., 1997), or we adopt the use of a relatively high protein dielectric constant (4–20 or higher) (Gilson and Honig, 1986; Antosiewicz et al., 1994; Demchuk and Wade, 1996; Warshel and Papazyan, 1998) whose theoretical justification is not entirely clear. This moderately high dielectric response of the protein region seems to help compensate for the rigidity imposed on the structure and is useful in semirigid MM-based calculations (Warshel and Åqvist, 1991). Obviously, large conformational changes cannot be properly modeled with this approach, especially if they result from charge-induced reorganization (small conformational fluctuations are probably reasonably accounted for by the use of a relatively high dielectric constant for the protein); unfortunately, this is a problem that also afflicts the aforementioned partially rigid MM-based methods. Despite this conformational problem and the somewhat empirical parameterization associated with it, the CE treatment seems to capture many of the important features of electrostatic free energy changes. Many satisfactory CE calculations have been made of (relative) redox potentials (Bashford et al., 1988; Gunner and Honig, 1991; Soares et al., 1997) and pK_a values (Bashford and Karplus, 1990; Bashford and Gerwert, 1992; Bashford et al., 1993; Yang et al., 1993; Demchuk and Wade, 1996) in proteins, and these calculations seem to be the only feasible route to the study of electron-proton coupling including the full protonation equilibrium (Lancaster et al., 1996; Soares et al., 1997; Kannt et al., 1998; Martel et al., 1999), even if that implies sacrificing some configurational aspects (of both the protein and the solvent). Obviously, only equilibrium thermodynamic aspects of the coupling can be analyzed.

The CE studies of electron-proton coupling have so far investigated either the effect of the redox state on CE-based pK_a calculations (Lancaster et al., 1996; Soares et al., 1997; Kannt et al., 1998) or, conversely, the effect of the protonation state on CE calculations of redox potentials (Martel et al., 1999). Hence, although the energetics were always treated within the CE framework, the weighting of states was not done in an integrated way. The primary aim of this work is to extend the weighting of states to CE redox calculations and, more importantly, to integrate the simultaneous weighting of the states of protonatable and redox sites. By reflecting both the pH and electrostatic potential of the solution, this is the procedure that most realistically reproduces the actual conditions in most in vitro and some in vivo studies. This type of approach makes it possible to analyze couplings between sites, including electron-proton coupling, in a way superior to the usual "static" approach based on direct interactions. It also makes it possible to analyze binding fluctuations and their possible role in in vivo transfer processes.

From a thermodynamic standpoint there are two main reasons to include weighting of states when treating the equilibrium of ligand binding in general. The first is concerned with the inability of a single state to reproduce the average effect of the ligands; e.g., the energetic effect of a site whose mean occupation is 0.5 obviously cannot be reproduced by considering the site to be either empty or occupied. But another, more subtle reason does exist: like the deconstraining of any other extensive property (e.g., energy), the deconstraining of the number (and position) of ligands creates an additional source of entropic effects. This new entropic term does not arise from protein or solvent configurational changes that may occur upon binding, which also contribute to the overall entropy, but rather from the empty/occupied fluctuations of the binding sites. Formally, the new entropic term is identical to the entropy of a system whose energetic states correspond only to different occupation states of its sites (i.e., a system without different configurational energy states for the protein and solvent; see below), so that it may be called occupational entropy. The change in occupational entropy in some processes may be an important fraction of the total entropy, so it can be misleading to establish a necessary association between entropy and configuration, as in the entropy interpretation proposed for *c*-type cytochromes by Bertrand et al. (1995), in terms of solvent configurational changes. In particular, occupational entropy may contribute significantly to the E^{half} or pK^{half} of a site, because the change of the occupation state of that site can affect the occupation states of neighboring sites. If the equilibrium of redox sites is not treated explicitly, as is usually done in "static" CE redox calculations, their contribution to the occupational entropy is entirely lost. The secondary aim of the present work is to compute some of these occupational entropy contributions for the selected model system and infer from the general magnitudes whether they can play an important role in redox and protonation equilibria in general.

One system in which the redox-Bohr effect has been well characterized (mostly in terms of equilibrium thermodynamic properties) is the tetraheme cytochrome c_3 of *Desulfovibrio* spp. (Santos et al., 1984; Coletta et al., 1991; Salgueiro et al., 1994, 1997; Turner et al., 1994, 1996; Park et al., 1996). These sulfate-reducing bacteria have the ability to use H_2 as the sole energy source when in the presence of sulfate (Badziong et al., 1978; Badziong and Thauer, 1978), and cytochrome c_3 is proposed to be involved in the sulfate reduction pathway, possibly by acting as a mediator between a periplasmic hydrogenase and transmembrane proteins that would pass electrons to the cytoplasm, where the reduction pathway takes place (Louro et al., 1996, 1997); the two electrons from H_2 oxidation are probably transferred simultaneously, eventually together with the two protons (Louro et al., 1996, 1997). The structure of cytochrome c_3 has been determined for several *Desulfovibrio* species (Higuchi et al., 1984; Matias et al., 1993, 1996; Czjzek et al., 1994; Morais et al., 1995) showing a generally conserved structure with four heme groups with bis-histidinyl axial coordination. The presence of several redox centers in such a small protein (13.5–15 kDa), displaying the redox-Bohr effect, makes cytochrome c_3 an ideal model system for the theoretical study of electron-proton coupling. In this work we have chosen cytochrome c_3 from *D. vulgaris* Hildenborough (DvHc_3) as a case study. Experimental (Saraiva et al., 1998; Messias et al., 1998) and theoretical (Soares et al., 1997, 1998; Martel et al., 1999) studies of DvHc_3 made so far seem to indicate propionate D of heme I as the protonatable site more strongly involved in the redox-Bohr effect, although other sites (His^{67}, N-terminus, propionate D of heme IV) also seem to be involved in the effect; these characteristics seem to be generally preserved in other *Desulfovibrio* species (Martel et al., 1999).

In the present work we start by presenting the theoretical basis for the treatment of the simultaneous binding equilibrium of protonatable and redox sites, as well as its consequences for the general concept of coupling between different binding sites; the concept of occupational entropy is also discussed. We then present an application of the proposed methodology to DvHc_3, aimed at complementing studies using other approaches (Soares et al., 1997, 1998; Martel et al., 1999); the study also serves as an illustration of the potential of the method. We analyze the equilibrium of electron and proton binding in this protein, in particular the question of electron-proton coupling and the molecular basis of the redox-Bohr effect. A major result of the study is the correct prediction of the complete heme order in the reduction pathway of DvHc_3, which was not possible with previous "static" calculations. Site-site couplings are then analyzed in terms of "dynamical" equilibrium quantities (correlations), instead of the usual and more limited "static" analysis based on direct interaction (free) energies. The involvement of protonatable sites in the biological redox-Bohr effect is studied, and the results seem to corroborate previous work. The concerted transfer of electrons and protons is also discussed and analyzed in terms of binding fluctuations. Finally, the contribution of occupational entropies to E^{half} and pK^{half} values (which is necessarily absent from the usual "static" calculations) is examined, and its magnitude is found to be significant. This application also shows that, by establishing a more direct and realistic connection to experimental parameters, the new proposed method leads to results whose analysis is both much simpler (no subjective choices of binding states are necessary) and complete (all energetic and entropic factors are taken into account) than the one possible by the usual methods.

THEORY

Binding equilibrium

The binding state of a protein with s binding sites can be represented by a vector $\mathbf{n} = (n_1, n_2, \ldots, n_s)$, where $n_i = 0$ or 1, depending on whether site i is empty or occupied. The probability of occurrence of (or the fraction of molecules

with) a binding state **n**, in conditions of thermodynamic equilibrium, is then given by

$$p(\mathbf{n}) = \frac{\exp[-\beta\Delta G(\mathbf{n})]\prod_i a_i^{n_i}}{\sum_{\mathbf{n}'}\{\exp[-\beta\Delta G(\mathbf{n}')]\prod_i a_i^{n'_i}\}}, \quad (1)$$

where $\Delta G(\mathbf{n})$ is the standard Gibbs free energy of the reaction whereby the protein changes from fully empty to the state **n**, a_i is the activity of the ligand species that binds to site i, and $\beta = 1/(kT)$, where k is Boltzmann's constant and T is the absolute temperature. This equation or similar ones can be derived from statistical mechanical or chemical equilibrium principles (e.g., Hill, 1960; Ben-Naim, 1992; Wyman, 1964; Schellman, 1975). If we define a quantity $pL_i = -\log_{10} a_i$, in analogy to the definition of pH, we can rewrite the probability of **n** as

$$p(\mathbf{n}) = \frac{\exp[-\beta\Delta G(\mathbf{n}) - 2.3\mathbf{n}\cdot\mathbf{pL}]}{\sum_{\mathbf{n}'}\exp[-\beta\Delta G(\mathbf{n}') - 2.3\mathbf{n}'\cdot\mathbf{pL}]}, \quad (2)$$

where $\mathbf{pL} = (pL_1, pL_2, \ldots, pL_s)$, and 2.3 stands for ln 10. In the present case we want to apply this general equation to the particular situation in which we have only two kinds of site: protonatable and redox. For protonatable sites one simply has $pL_i = pH$. For redox sites the reactions of interest correspond to the "half-cell" reduction reactions, so that, strictly speaking, the redox part of $\Delta G(\mathbf{n})$ should be considered relative to the standard hydrogen electrode potential. In fact, it is convenient for implementation purposes (see below) to adopt an oxidation-based instead of a reduction-based formalism, i.e., the state $n_i = 1$ will correspond to the oxidized state. Thus, for oxidizable (instead of reducible) sites we have to set $pL_i = -eE/(2.3kT)$, where e is the protonic charge and E is the electrostatic potential of the solution (or, more exactly, the difference in electrostatic potential between the electrodes). This convention, whereby we regard oxidation as the occupation of sites by a positive charge e, is a formal convenience that does not affect the validity of Eq. 2.

If we have a method for computing the $\Delta G(\mathbf{n})$ values, Eq. 2 can be used directly to perform a sampling of the states **n**, using, e.g., an MC method (Antosiewicz and Porschke, 1989; Beroza et al., 1991; Yang et al., 1993). To perform a full study of the relevant external parameters, we have to scan both the pH and potential of the system and simultaneously sample the protonable and redox sites, using a "two-way" MC scheme like the one described in the Methods section. The $\Delta G(\mathbf{n})$ values can in principle be obtained by considering a thermodynamic cycle involving model compounds (Warshel, 1981; Bashford and Karplus, 1990), as long as we can compute the free energy changes of the reactions $\mathbf{0} \rightarrow \mathbf{n}$ in both the protein and the set of model compounds. As discussed in the Introduction, CE methods are the only feasible approach to such a large number of states, as in pK_a calculations; this methodology is discussed in the Methods section.

Coupling between sites

One way of measuring the coupling between sites is to analyze the magnitudes of their interaction (free) energies, because this gives a measure of how much a change in the binding state of one site perturbs the binding state of the other in a direct way. Thus the coupling between sites, and in particular of electron-proton couplings, is usually analyzed in terms of these direct interactions (Lancaster et al., 1996; Soares et al., 1997; Kannt et al., 1998).

The direct interaction is obviously an important contribution to the coupling between two sites (and probably the determinant one in many cases), but this "static" approach neglects the existence of indirect effects through other sites whose binding states may change in a concerted and complex manner (allostery is another, more familiar source of indirect effects). The tendency of two sites to have either identical or opposed binding states is determined by both the direct and indirect effects between them, and by looking only at the former we can lose important information, as the following simple example illustrates. Consider a three-site system in which site 1 has strong destabilizing interactions with sites 2 and 3, which in turn have a weaker destabilizing interaction between them. When the ligand activity is high enough to induce doubly occupied states, the simultaneous occupation of sites 2 and 3 is obviously the preferred one; hence, those two sites will tend to have the same binding state, even though their direct interaction is destabilizing. The existence of this particular doubly occupied state, which may be involved in the biological function of the system, originates from indirect effects and could not have been suspected from their destabilizing direct interaction alone; instead of looking at isolated direct interactions, one has to look at the set of all direct interactions (as well as the intrinsic affinities) and calculate the resulting equilibrium and correlations. This simple example illustrates the importance of including indirect effects when analyzing the effective coupling between two sites and suggests that a more appropriate measure for that coupling is the statistical correlation between their binding states. This correlation is given for a pair of sites (i, j) as a function of the variances and covariance of their binding states (Mood et al., 1974):

$$\rho_{ij} = \frac{\mathrm{cov}(n_i, n_j)}{[\mathrm{var}(n_i)\mathrm{var}(n_j)]^{1/2}}. \quad (3)$$

Of course, the correlation between two sites is not a constant of the system, as the direct interaction, but rather a function of its thermodynamic state; in the case of interest to us here, the correlation between any pair of sites will be a function of pH and E (and the temperature).

The analysis of coupling between sites based on statistical correlations is not limited to pairs of sites, but can also be applied to measure the coupling between groups of sites; in particular, it can measure the coupling between total protons and total electrons. This is simply an alternative way of looking at the traditional concept of linkage (Wyman, 1964) (the so-called linkage relation is a statement

about two alternative ways of computing the covariance of the total numbers of different ligand types).

In general, this type of coupling analysis based on correlations, which is superior to the usual one based on direct interactions, is only possible when the full redox and protonation equilibria are considered, as in the method proposed here.

Occupational entropy

The statistics obtained from the sampling of binding states provide a route for computing various equilibrium thermodynamic properties, including the occupational entropies mentioned in the Introduction. The complete specification of the microstate of the protein system comprehends its binding state **n** and its configurational state Γ (the configurational state is here understood as the coordinates and momenta of the protein and surrounding solvent). The entropy of this system can be written as (Hill, 1960)

$$S = -k \sum_{\mathbf{n}} \sum_{\Gamma} p(\Gamma, \mathbf{n}) \ln p(\Gamma, \mathbf{n}), \tag{4}$$

where $p(\Gamma, \mathbf{n})$ is the probability of state $(\Gamma, \mathbf{n})$; the states Γ are considered discrete for simplicity of notation. It should be noted that the order of the sums is significant, because **n** does in general determine the number and specification of the degrees of freedom included in Γ (because of the binding protons). This entropy can be alternatively written as

$$\begin{aligned} S &= -k \sum_{\mathbf{n}} \sum_{\Gamma} p(\Gamma|\mathbf{n}) p(\mathbf{n}) [\ln p(\Gamma|\mathbf{n}) + \ln p(\mathbf{n})] \\ &= \langle S(\mathbf{n}) \rangle - k \sum_{\mathbf{n}} p(\mathbf{n}) \ln p(\mathbf{n}), \end{aligned} \tag{5}$$

where $p(\Gamma, \mathbf{n})$ is the conditional probability of Γ for a given **n**, and $p(\mathbf{n})$ is the total (configuration-independent) probability of state **n**; the angle brackets denote the average over all **n** states, and

$$S(\mathbf{n}) = -k \sum_{\Gamma} p(\Gamma|\mathbf{n}) \ln p(\Gamma|\mathbf{n}) \tag{6}$$

is the entropy of a system with the fixed binding state **n**. The first term of Eq. 5 is the average of the entropy of the constant-**n** system, exclusive of configurational origin, and can thus be called configurational entropy:

$$S^{\text{conf}} = \langle S(\mathbf{n}) \rangle. \tag{7}$$

The second term is formally identical to the entropy of a hypothetical system whose microstates differ by the occupation states of the binding sites but have the same energy; hence this term may be called occupational entropy:

$$S^{\text{occ}} = -k \sum_{\mathbf{n}} p(\mathbf{n}) \ln p(\mathbf{n}). \tag{8}$$

Thus we can write

$$S = S^{\text{conf}} + S^{\text{occ}}. \tag{9}$$

We note that this decomposition of the entropy does not result from a convenient but nevertheless arbitrary separation of degrees of freedom, as is often the case (e.g., the translational, rotational, and vibrational entropies of an ideal polyatomic gas), but rather from the actual thermodynamic effect of binding equilibrium. This aspect can be better understood if we try to estimate the entropy of the system using a single, even if representative, binding state **n***. The entropy of this representative state **n*** may be a very good estimate of the configurational entropy of the system in binding equilibrium, i.e., $S(\mathbf{n}^*) \approx \langle S(\mathbf{n}) \rangle$, but it totally misses the additional occupational term. This actually illustrates the more general fact that the act of deconstraining an extensive thermodynamic parameter has a twofold entropic effect: it averages the constrained-system entropy over the new available states and introduces a new entropy term due to the fluctuations of the newly deconstrained parameter. If we interpret the entropy in terms of the fluctuations of the system microstates, S^{occ} reflects the empty/occupied fluctuations of the binding sites ($n_i = 0/1$), much in the same way as the more familiar $S(\mathbf{n})$ reflects the fluctuations of the protein and solvent configurations. In fact, the consideration of the binding equilibrium leads in general to increased fluctuations in all microscopic properties of the system, when compared to the situation in which a single representative binding state **n*** is considered (Baptista et al., 1997); again, this is generally valid for the deconstraining of any extensive thermodynamic parameter. These considerations show that the use of discrete redox states adopted in "static" CE redox calculations (Lancaster et al., 1996; Soares et al., 1997; Kannt et al., 1998; Martel et al., 1999) misses entirely the contribution of redox site fluctuations to the occupational entropy, which should be present in any free energy term computed.

The contribution of the occupational entropy to the free energy change of a process is a measure of how much the fluctuations of the states n_i are altered by the change in question. In particular, the process of occupying a previously empty site will in general affect the occupational fluctuations of the remaining sites, meaning that the entropic contribution to the E^{half} or pK^{half} value of a given site is not necessarily configurational, as is often assumed (Bertrand et al., 1995). The standard free energy change of the reaction of binding to site *i* is given by

$$\Delta G_i = -2.3kT\text{p}L_i - kT \ln \frac{\langle n_i \rangle}{1 - \langle n_i \rangle}. \tag{10}$$

For a protonatable site, ΔG_i corresponds to the effective pK_a of site *i*, $\Delta G_i = -2.3kT\text{p}K_i^{\text{eff}}$, and Eq. 10 is the Henderson-Hasselbalch equation. For a redox site, ΔG_i corresponds to the effective potential of site *i*, $\Delta G_i = eE_i^{\text{eff}}$ (because ΔG_i refers to oxidation) and Eq. 10 is the Nernst equation. The

free energy ΔG_i can be written in terms of its contributions as

$$\Delta G_i = \Delta H_i - T\Delta S_i = \Delta H_i - T\Delta S_i^{conf} - T\Delta S_i^{occ}, \qquad (11)$$

where ΔS_i^{occ} can be computed in terms of the microscopic binding statistics (see Appendix):

$$T\Delta S_i^{occ} = kT \ln \frac{\langle n_i \rangle}{1 - \langle n_i \rangle} + \frac{\mathrm{cov}[n_i, \Delta G(\mathbf{n}) + 2.3kT\mathbf{n} \cdot \mathbf{pL}]}{\mathrm{var}(n_i)}. \qquad (12)$$

Hence it is possible to compute ΔG_i and its contributions ΔS_i^{occ} and $\Delta H_i - T\Delta S_i^{conf}$, solely from the binding statistics.

From a computational point of view, and as noted in the Introduction, the CE approach used here can only perform an approximated configurational averaging, especially for the protein conformation, where at best the averaging reflects small-scale fluctuations of the conformation used; this will necessarily affect the occupational entropies computed. The protein conformation in a binding system can, in principle, be explicitly treated along the line presented by Baptista et al. (1997), with consequent improvements in occupational entropy calculations, but such an approach is far too demanding for the full analysis intended in this work.

METHODS

Model structure

The structure of DvHc_3 used for the calculations was the one published by Matias et al. (1993), with PDB code 1cth, more precisely molecule A of the asymmetrical unit. Crystallographic water molecules were discarded. This structure was obtained under oxidizing conditions and may not be fully representative of more reduced states.

The choice of coordinates for polar and aromatic hydrogen atoms is an important aspect in CE calculations, because incorrect placement may lead to incorrect hydrogen-bond networks or even to atomic overlap for some protonation states (Alexov and Gunner, 1997). Hydrogen atoms were added in several stages. First, hydrogen atoms that are covalently nonambiguous and have a unique conformation were added using GROMOS 87 (van Gunsteren and Berendsen, 1987), considering explicit polar and aromatic hydrogens (Smith et al., 1995). Next, this structure was used to add hydrogen atoms that are covalently nonambiguous but have a variable conformation; this was done using the program WHATIF (Vriend, 1990), which implements an empirical potential for hydrogen bonding and optimization methodologies for hydrogen-bond networks (Hooft et al., 1996). Finally, with the structure thus obtained, this same procedure was used to add hydrogen atoms that are covalently ambiguous and correspond to the titrating protons of carboxylic groups. The positioning of the hydrogen atoms obtained in this last stage was subsequently checked by visual inspection of hydrogen-bonding patterns and corrected when found necessary; in particular, all four different positions in the carboxylic plane were considered, whereas WHATIF only considers the two extended ones.

Continuum electrostatic calculations

After building of the DvHc_3 structure as described above, CE calculations were made using Donald Bashford's software package MEAD (Bashford and Gerwert, 1992), the methodology of which is based on a thermodynamic cycle involving protein and model compounds and has been described elsewhere (Warshel, 1981; Bashford and Karplus, 1990). Although this software was originally developed for the treatment of protonatable sites, the treatment of oxidizable sites is formally identical, as discussed in the Theory section. MEAD assumes that a positive charge is added upon binding, so that the redox process has to be expressed in terms of oxidizable instead of reducible sites (see the Theory section). These oxidizable sites can then simply be included in the set of protonable sites given as input to MEAD, classified as cationic (thus, their "neutral" state is the reduced form).

The consideration of the thermodynamic cycle involving model compounds requires a specification of the structures of these compounds. In MEAD the model compounds of amino-acidic sites are obtained by "carving out" from the protein the *N*-formyl-*N*-methylamide derivative of the amino acid residue where the site is located. In the case of propionate sites the model compound was taken as the corresponding acetyl group. The model compound of the heme sites consists of the heme group, excluding the atoms used in the model compound of the propionates, plus the side chains of the axial histidines, and the C_β and S_γ atoms of the attached cysteines.

For each site *i* MEAD requires a pK_i^{mod} value, which originally corresponds to the pK_a of its model compound in solution. The pK^{mod} values for the usual amino-acidic protonable sites were taken from Nozaki and Tanford (1967) and the value for propionate sites was taken as the pK_a of acetic acid (Weast, 1984); these are shown in Table 1. In the case of redox sites the pK_i^{mod} should correspond to the reduction potential of the model compounds used in the calculations, more precisely to $-eE_i^{mod}/(2.3kT)$ (because they are oxidizable sites). In the present case, the model compound of the heme sites does not correspond to a real

TABLE 1 pK^{mod} values for protonatable sites

Site	pK^{mod}
Arginine	12.0
Lysine	10.4
Tyrosine	9.6
N-terminus	7.5
Histidine	6.3
Propionate	4.75
Aspartate	4.0
Glutamate	4.4
C-terminus	3.8

molecule whose potential can be determined or estimated easily. A reduction potential of −220 mV has been measured for an octapeptide bis-histidinyl derivative of the heme of cytochrome *c*, at pH 7 (Harbury et al., 1965). Because our model compound has the heme more exposed to the solvent than this derivative, its more strongly charged form (the oxidized one) is in principle more stable; the propionate sites, although probably ionized at pH 7, are probably too strongly solvated to have a significant effect. Hence we expect a reduction potential slightly more negative than −220 mV. In any case, because all redox sites are of the same type, with the same E_i^{mod} value, we can simply set this value equal to zero and consider all potentials as relative to this reference value, instead of the value of the standard hydrogen electrode. The standard reduction potential of our model compound can be determined a posteriori by comparison with experiment (see below).

The set of charges for the protonatable sites was taken or adapted from the GROMOS 87 force field (van Gunsteren and Berendsen, 1987) with polar and aromatic hydrogens (Smith et al., 1995). Because all titrating protons have been positioned in the structure (see above), we can describe the deprotonated/protonated change as the addition of an explicit hydrogen atom. In some cases this is highly desirable, such as when one of the oxygen atoms of a carboxylic group is establishing hydrogen bonds with other groups and the other oxygen atom is free; in this case the proton should be added to the free oxygen atom. However, there are cases in which such an approach represents no advantage, as in the case in which titrable sites are totally exposed and are not establishing any obvious interaction with other groups. In this case, an average description of the deprotonated/protonated change may be more adequate. For this reason, a choice of average or explicit protonation was made based on visual inspection for Asp, Glu, Tyr, and propionate sites. All other titrable sites had an average description of protonation, which corresponds to always (never) using the positions of the titrating protons for cationic (anionic) sites; in these cases the titration corresponds only to a change on the partial charges of permanent atoms. The atomic partial charges used for cationic and anionic sites are shown, respectively, in Tables 2 and 3. The atomic partial charges for the heme sites were obtained from quantum chemical calculations, as described elsewhere (Martel et al., 1999), and are shown in Table 4.

The dielectric boundary between the protein cavity and the solvent is computed by MEAD by rolling a spherical probe over the protein molecular surface. The protein atomic radii defining the molecular surface were taken to be half of the minimum energy distance between like-atom pairs in the GROMOS 87 force field (van Gunsteren and Berendsen, 1987). The solvent probe radius was 1.4 Å, which should be a reasonable spherical approximation of the water molecule, and the ionic exclusion layer thickness was set at 2.0 Å, which approximates the sizes of counterionic species in physiological conditions (Gilson and Honig, 1988). The dielectric constant used for the solvent region was 80, the approximate value for bulk water at room temperatures. The dielectric constant for the protein interior was chosen as 15, based on previous studies with this same protein (Soares et al., 1997; Martel et al., 1999), in consonance with suggestions by other workers (Antosiewicz et al., 1994; Demchuk and Wade, 1996). As noted in the Introduction, the use of moderately high values for the inner dielectric constant is supposed to reflect the effect of conformational fluctuations, even though the question remains on empirical grounds. The ionic strength used in the calculations was 0.1 M, a value approaching the in vivo values, and the temperature was 300 K.

MEAD uses a finite-difference technique to solve the linear Poisson-Boltzmann equation. A two-step focusing method (Gilson et al., 1987) was used: a first calculation

TABLE 2 Atomic partial charges for cationic sites

Atom name	Partial charge	
	Prot.	Deprot.
Arginine		
CB	0.000	0.000
CG	0.000	0.000
CD	0.090	0.000
NE	−0.110	−0.150
HE	0.240	0.150
CZ	0.340	0.200
NH1	−0.260	−0.400
HH11	0.240	0.150
HH12	0.240	0.150
NH2	−0.260	−0.400
HH21	0.240	0.150
HH22	0.240	0.150
N-terminus		
CB	0.000	0.000
CA	0.127	0.000
N	0.129	−0.840
H1	0.248	0.280
H2	0.248	0.280
H3	0.248	0.280
Lysine		
CB	0.000	0.000
CG	0.000	0.000
CD	0.000	0.000
CE	0.127	0.000
NZ	0.129	−0.840
HZ1	0.248	0.280
HZ2	0.248	0.280
HZ3	0.248	0.280
Histidine		
CB	0.000	0.000
CG	−0.050	0.130
ND1	0.380	−0.580
HD1	0.300	0.000
CD2	0.000	0.000
HD2	0.000	0.000
CE1	−0.240	0.260
HE1	0.000	0.000
NE2	0.310	0.000
HE2	0.300	0.190

TABLE 3 Atomic partial charges for anionic sites

Atom name	Partial charge Prot.	Partial charge Deprot.
Tyrosine		
CB	0.000	0.000
CG	0.000	0.000
CD1	−0.100	−0.100
HD1	0.100	0.100
CD2	−0.100	−0.100
HD2	0.100	0.100
CE1	−0.100	−0.100
HE1	0.100	0.100
CE2	−0.100	−0.100
HE2	0.100	0.100
CZ	0.150	−0.200
OH	−0.150	−0.800
	−0.548*	
HH	0.000	0.000
	0.398*	
Aspartate		
CB	0.000	0.000
CG	0.530	0.270
OD1	−0.265	−0.635
	−0.380*	
OD2	−0.265	−0.635
	−0.548*	
HD2	0.000	0.000
	0.398*	
Glutamate		
CB	0.000	0.000
CG	0.000	0.000
CD	0.530	0.270
OE1	−0.265	−0.635
	−0.380*	
OE2	−0.265	−0.635
	−0.548*	
HE2	0.000	0.000
	0.398*	
Propionate		
CBA	0.000	0.000
CGA	0.530	0.270
O1A	−0.265	−0.635
	−0.380*	
O2A	−0.265	−0.635
	−0.548*	
HO2A	0.000	0.000
	0.398*	
C-terminus		
CT	0.530	0.270
O1	−0.265	−0.635
O2	−0.265	−0.635

*Charges for explicit protonation.

TABLE 4 Atomic partial charges for heme sites

Atom name	Partial charge Oxidized	Partial charge Reduced
Heme core		
FE	1.200	1.200
NA	−0.390	−0.405
NB	−0.390	−0.390
NC	−0.380	−0.405
ND	−0.400	−0.400
CHA	−0.085	−0.085
HCHA	0.120	0.095
C1A	0.110	0.040
C2A	0.000	0.000
C3A	−0.015	−0.055
C4A	0.110	0.110
CMA	0.035	−0.010
CAA	0.020	−0.005
CHB	−0.080	−0.140
HCHB	0.080	0.045
C1B	0.100	0.100
C2B	0.000	−0.040
C3B	−0.040	−0.040
C4B	0.090	0.030
CMB	0.035	−0.010
CAB	−0.070	−0.070
CBB	0.035	0.015
CHC	−0.100	−0.100
HCHC	0.070	0.045
C1C	0.090	0.040
C2C	−0.010	−0.010
C3C	−0.020	−0.055
C4C	0.105	0.105
CMC	0.020	−0.010
CAC	−0.065	−0.065
CBC	0.035	0.010
CHD	−0.090	−0.145
HCHD	0.080	0.045
C1D	0.110	0.110
C2D	−0.010	−0.050
C3D	0.000	0.000
C4D	0.100	0.025
CMD	0.050	0.000
CAD	0.020	−0.005
Cys attached to ring B		
CB	−0.070	−0.070
SG	0.130	0.110
Cys attached to ring C		
CB	−0.070	−0.070
SG	0.140	0.110
Axial histidines		
CB	0.005	0.005
CG	0.110	0.110
ND1	−0.305	−0.305
HD1	0.260	0.260
CD2	0.000	0.000
HD2	0.100	0.100
CE1	0.195	0.195
HE1	0.140	0.140
NE2	−0.305	−0.305

using a (80 Å)^3 cube with a 1.0-Å lattice spacing, centered on the protein, followed by a second calculation using a (20 Å)^3 cube with a 0.25-Å spacing, centered on the titrable site; for the model compounds calculations, the sides of the cubes were, respectively, 60 Å and 15 Å.

As output MEAD produces a set of intrinsic pK_a values, $\{pK_i^{int}\}$, and a matrix of site-site interaction energies, $\{W_{ij}\}$. In the case of protonatable sites, pK_i^{int} stands for the intrinsic pK_a of site i when all other sites $j \neq i$ are in their "neutral" state (the reduced state for redox sites, because they are treated as cationic); for redox sites it corresponds to the

intrinsic reduction potential E_i^{int} in the "neutral" environment, and more exactly to $-eE_i^{int}/(2.3kT)$. The pairwise term W_{ij} is the site-site interaction between *i* and *j*, more exactly the difference between the electrostatic energies of the like pairs (0,0) and (1,1), and those of the cross-pairs (0,1) and (1,0). These two sets of values contain all of the information necessary to compute the populations of binding states of the protein (see below).

Monte Carlo calculations

As discussed above, redox sites can be easily included in the formalism of protonatable sites. Hence, as can be shown from the formalism of the Theory section, the probability of state **n** can simply be written as a generalization of the expressions previously derived by other workers for the protonation case (Tanford and Kirkwood, 1957; Bashford and Karplus, 1990; Yang et al., 1993):

$$p(\mathbf{n}) = \frac{\exp^{[2.3\,\Sigma_i\, n_i(\mathrm{p}K_i^{int} - \mathrm{pL}_i) - \beta\,\Sigma_i\,\Sigma_{j<i}\, z_i(n_i) z_j(n_j) W_{ij}]}}{\sum_{\mathbf{n}'} \exp^{[2.3\,\Sigma_i\, n'(\mathrm{p}K_i^{int} - \mathrm{pL}_i) - \beta\,\Sigma_i\,\Sigma_{j<i}\, z_i(n_i') z_j(n_j') W_{ij}]}}. \qquad (13)$$

This equation provides the base for the MC calculations. The pK_i^{int} and W_{ij} values are computed by MEAD, as discussed above. The quantity $z_i(n_i)$ stands for the change (in protonic units) of site *i* with respect to the "neutral" form: $z_i(n_i) = z_i(0) + n_i$, with $z_i(0) = -1$ for anionic sites and 0 for cationic and redox ones.

For the sampling of binding states we have implemented an MC method that follows the Metropolis criterion to accept or reject trial modifications of state (Metropolis et al., 1953). The trial modifications consist of flips of the state of binding sites, $0 \leftrightarrows 1$, which automatically ensures that the stochastic matrix of trial moves is symmetrical, as required by the Metropolis algorithm (Allen and Tildesley, 1987). To avoid "bottlenecks" in binding space, where the system may become trapped, double flips were attempted for pairs of strongly coupled sites ($W_{ij} \geq 2$ pH units), as done by Beroza et al. (1991). Instead of random selection of individual and paired sites, and to speed up calculations, trial flips were sequentially attempted for all individual sites and pairs; this also corresponds to a valid Markov chain, leading to a proper sampling of the binding states (Hastings, 1970).

In usual calculations for protonatable sites, several MC runs are made within the pH range of interest. In the present case a grid of pH versus *E* (electrostatic potential) has to be considered instead. A main calculation was made in which the pH was varied from -5 to 25 in steps of 0.2, and *E* was varied from -500 mV to 500 mV in steps of 10 mV (relative to the E^{mod} value of the heme sites; see above); the temperature was 300 K. Each MC run consisted of 40,000 steps, and each step was defined as a full cycle of trial flips over the lists of individual and paired sites. Because the errors in fluctuations and correlations are always larger than those of average values, longer runs were made to compute properties involving those quantities, for selected values of pH and *E*; fluctuations and occupational entropies were computed using 2×10^5 steps, and site-site correlations using 10^6 steps.

RESULTS AND DISCUSSION

Redox titration

Because two thermodynamic parameters are being examined simultaneously, pH and electrostatic potential *E*, the titration behavior of the system is fully represented by titration surfaces instead of curves.

The total redox titration surface of c_3DvH, shown in Fig 1 *a*, displays a marked dependence on pH. The titration curves (i.e., the lines parallel to the *E* axis) are shifted to more positive *E* values as the pH decreases. This type of shift is what should be expected on electrostatic grounds: a lower pH means a tendency of the protonatable sites to be occupied, increasing the overall charge of the protein and thus facilitating the binding of electrons, so that reduction can occur at higher *E* values. The resulting sideways shift on

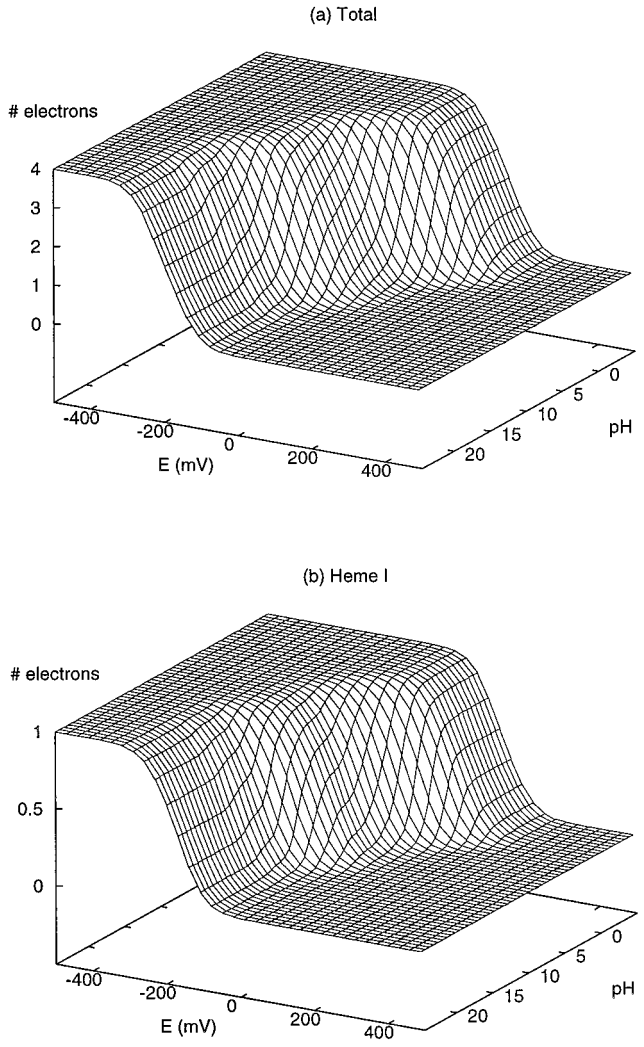

FIGURE 1 Redox titration surfaces for the total protein (*a*) and heme I (*b*).

the titration surface is the signature of the redox-Bohr effect. A more careful examination of the surface shows that several shifts occur: two pronounced shifts, in the pH ranges 1–8 and 10–15, and a much smaller one around pH 17. As will be seen below, these coincide with the regions where large protonation changes occur in the protein. This simply reflects the nonspecific chemical physical origin of the redox-Bohr effect alluded in the Introduction: whenever protonable and redox sites coexist in a protein, a thermodynamic coupling between them is to be expected because of the strength and long-range nature of electrostatic interactions. This will be more evident for redox sites, because they will usually have several neighboring protonatable sites that can affect them; because there are usually much fewer redox sites than protonatable ones, the effect may not be significant for many of the protonatable sites (see below).

The titration surfaces for the individual hemes are very similar to the surface of total titration; one of them is shown in Fig. 1 *b*. Although the exact location and extension of the shifts are slightly different for different hemes, they also occur at the pH regions of maximum protonation changes.

It should be noted that even though three shifts are present on the surfaces of Fig. 1, only one of them is of biological interest. The optimum pH for the growth of *D. vulgaris* is 6.5 (Badziong and Thauer, 1978), and a redox-Bohr effect on DvHc_3 is known to occur in the pH range 5–8 (Turner et al., 1996). Hence, only the first shift, in the pH range 1–8, should be of biological interest.

It is interesting to see how well the present calculation reproduces the experimental results at physiological pH. A direct comparison with experimental individual titration curves is not possible, but we can make the comparison with a simple binding model (1 protonable + 4 redox sites) by Turner et al. (1996); this model reproduces quite well the experimental data it was fitted to and can be used to obtain titration curves. A comparison between the titration curves of that model and our calculations, at pH 6.6, is shown in Fig. 2, *a* and *b*. The *E* scale of plot *b* has been shifted to obtain an optimal superposition of the total titration curves of both plots; our $E = 0$, which refers to the reduction potential of the heme model compound in solution (see Methods), is seen to correspond to a standard value (relative to the standard hydrogen electrode) of about -265 mV. This value is slightly more negative than the -220 mV measured for a similar model compound (Harbury et al., 1965), as expected from desolvation arguments (see Methods).

The calculated titration curves for individual hemes are ordered as the experimental ones, i.e., the present methodology predicts correctly the relative order of reduction of the four hemes of DvHc_3 at physiological pH. Nevertheless, some important differences exist, specially for hemes I and II. Besides being too far apart, the calculated titration curves of these two hemes show a much more gradual variation than those of plot *a*. The high steepness of the experimental curves reflects the positive cooperativity experimentally observed between hemes I and II (Turner et al., 1996). Given the repulsive nature of the electrostatic interactions

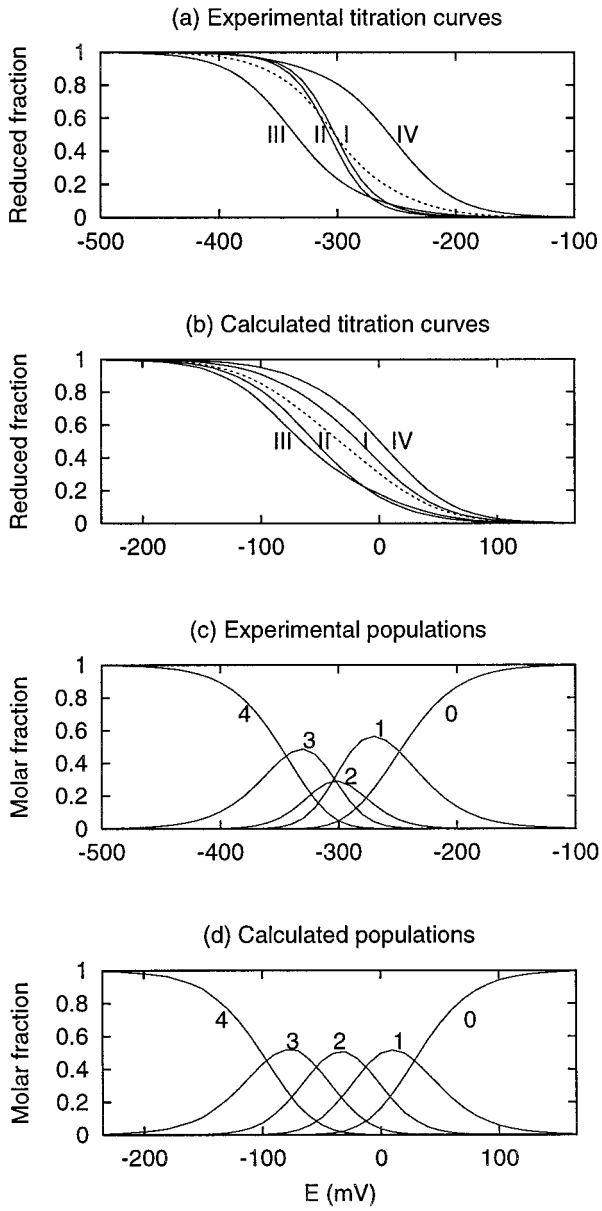

FIGURE 2 Comparison of experimental (*a, c*) and calculated (*b, d*) redox data for DvHc_3, at pH 6.6. (*a, b*) Titration curves of individual hemes (*labeled solid lines*) and the total protein (*dashed line*). (*c, d*) Populations of the molecules with 0–4 (heme-reducing) electrons.

between the sites, the most likely explanation for this behavior is the existence of an allosteric conformational change induced by the change in redox state of hemes I and/or II. The existence of reduction-induced conformational changes in DvHc_3 has recently been observed in a NMR structural study (Messias et al., 1998) and in a MD simulation study (Soares et al., 1998). Because the CE approach adopted here cannot account for conformational changes (except perhaps for small fluctuations; see the Introduction), it is not surprising that we fail to predict the positive cooperative behavior. The consequence of this failure is that, by missing the sudden and almost simultaneous reduction of the two hemes, we are assigning a too high

probability for molecules with two reduced hemes, as can be seen in Fig. 2, *c* and *d*; plot *c* refers again to the model by Turner et al. (1996) (where the molecules with 0–4 oxidized hemes are called *stages*). It is remarkable that even while missing this effect, the present methodology is able to predict the correct order of reduction for all four hemes, suggesting that the basic energetics of the system is satisfactorily described by the CE model. Of course, the excessive stabilization of molecules with two electrons in our calculations shows DvHc_3 to be less efficient in the uptake of two simultaneous electrons than it actually is. The evolutionary advantage of developing the supposed conformational change would have been the usual one for developing positive cooperativity: the fine-tuning of function within a very narrow range of physiological conditions.

A more synthetic way of expressing the effect of pH upon the redox titration of DvHc_3, and the usual way of characterizing the redox-Bohr effect, is in terms of the pH dependence of the E^{half} values. Fig. 3 *a* shows this dependence for the four heme sites; the curves correspond to the intersection of the individual titration surfaces (like the one in Fig. 1 *b*) with the plane $z = 0.5$. The largest shifts occur where large protonation changes take place, as expected from electrostatic effects and discussed above, apropos of the titration surfaces. This illustrates again the nonspecific nature of the redox-Bohr effect, which inevitably appears whenever redox and protonable sites coexist on the same molecule. The order of reduction of the four hemes in the pH range 5–8 is consistent with Fig. 2. The E^{half} curves cross each other several times within the whole pH range; in particular, the order of the curves at very low pH is precisely the opposite of that at very high pH. The large number of crossings in the plot indicates a close balance of effects, which, given the successful prediction of reduction order, seem to be properly captured by the present methodology.

In Fig. 3 *b* we show the curves resulting from the intersection of the total titration curve of Fig. 1 *a* with the planes $z = 1$, 2, and 3. These loci correspond to macroscopic states with an average number of (heme-reducing) electrons equal to 1, 2, and 3, respectively. These states, called M1–M3, are not the same as the molecular populations with 1–3 (heme-reducing) electrons mentioned above, but have the advantage of being truly macroscopic and therefore more easily related to the external parameters; the two types of state are actually closely related (as one may intuitively expect), because each E_{Mk} curve in Fig. 3 *b* coincides with the curve of maximum fraction of molecules with *k* (heme-reducing) electrons at the given pH (not shown). The potentials E_{Mk} can be regarded as a total-molecule counterpart of the E^{half} values. The states M*k* will be used below in the analysis of several properties of DvHc_3. The shifts in the E_{Mk} curves occur at the same regions as in plot *a*, just another manifestation of the redox-Bohr effect.

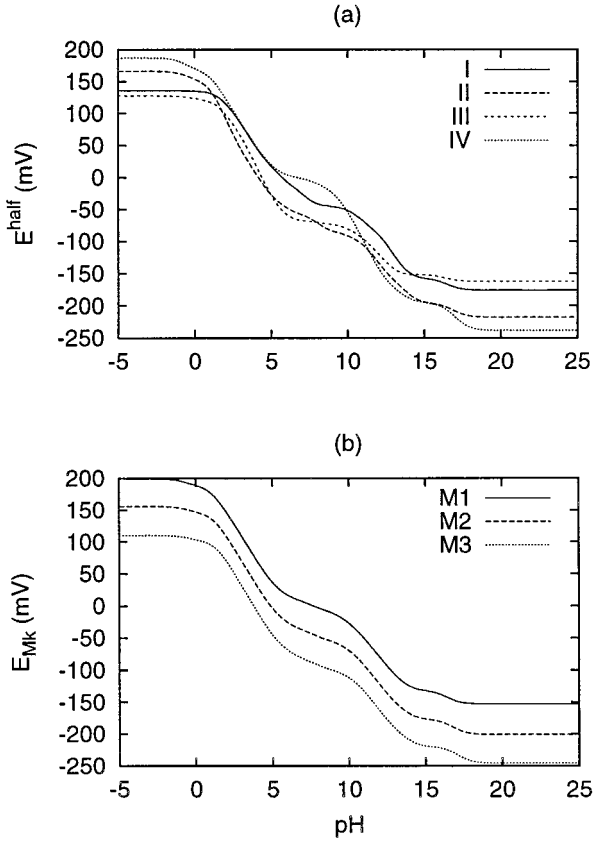

FIGURE 3 E^{half} values for individual hemes (*a*) and isoreduction curves corresponding to states M1–M3 (*b*), as a function of pH.

Proton titration

In contrast to the total redox titration curve, the total proton titration surface of c_3DvH, shown in Fig. 4 *a*, shows no evident signs of the redox-Bohr effect, looking virtually flat along the *E* axis. This is essentially due to the fact that of the 48 protonatable sites of the protein, only a few are close enough to the heme sites to be significantly affected by changes in their redox state; the variation in the total protonation is thus very small (see also Fig. 8 below and the discussion therein). To see these effects, one has to look at individual rather than total proton titration surfaces. One of the sites where this effect can be clearly seen is propionate D of heme I, the surface of which is shown in Fig. 4 *b*. The sideways shift seen on the surface is again the signature of the redox-Bohr effect, in this case from the standpoint of proton titration: the titration curves (i.e., the lines parallel to the pH axis) are shifted to lower pH values as *E* takes more positive values; the shift occurs between −100 mV and 100 mV. This type of shift is what should be expected on electrostatic grounds, because an increased *E* means a tendency of the hemes to be oxidized, making the binding of protons more difficult, which thus occurs at lower pH values. Several protonable sites exhibit this type of titration surface, in particular the propionate D of heme IV, whose surface is very similar to that of Fig. 4 *b* (not shown); less pronounced effects can be seen for other propionates. Of the remaining protonatable sites, only some should be biologi-

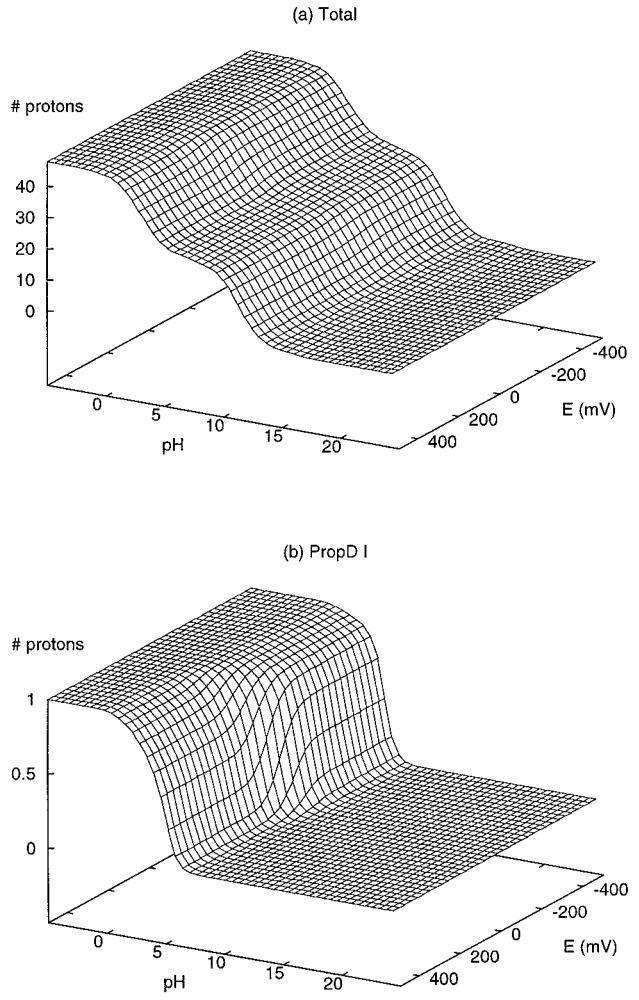

FIGURE 4 Proton titration surfaces for the total protein (*a*) and propionate D of heme I (*b*).

cally interesting. The optimum pH for the growth of *D. vulgaris* is 6.5 (Badziong and Thauer, 1978), and a redox-Bohr effect on DvHc_3 is known to occur in the pH range 5.0–8.0 (Turner et al., 1996). Thus, even though many protonatable sites may be coupled to redox changes, we will consider, in addition to the propionates, only the ones titrating in this pH range. These are His^{67} and the N-terminus, which show a small shift in their titration surfaces (not shown). Other protonatable sites whose titration is dependent on E (e.g., tyrosines) have their titration region too far from the biologically relevant region.

The dependence of proton titration on E can be represented in a more condensed form in terms of the E-dependent pK^{half} values of the protonatable sites; this is actually a common way of characterizing the redox-Bohr effect. This dependence is shown in Fig. 5 for the propionate sites, His^{67} and the N-terminus; the same y range was used in all plots for ease of comparison. The site showing a larger shift in the pH range 5–8 is propionate D of heme I, suggesting that this may be the protonatable site more strongly involved in the physiological redox-Bohr effect, in agreement with other theoretical (Soares et al., 1997; Martel et al., 1999) and experimental (Park et al., 1996; Saraiva et al., 1998; Messias et al., 1998) studies of *D. vulgaris* c_3. The propionate D of heme IV also shows a very large pK_a shift, even though it stays out of the 5–8 range. It is not surprising that the propionate sites show the highest shifts, given their proximity to the heme centers. The pK^{half} shifts for His^{67} and the N-terminus, although small, are within the pH range of the biological redox-Bohr effect. The shift of the N-terminus site may not be present in solution, because calculations done with the other molecule (B) of the asymmetrical unit show much lower values for its interaction with heme I (Soares et al., 1997), and the conformation of the N-terminal chain may be quite flexible.

Coupling between sites

From purely electrostatic arguments we expect the total number of protons and the total number of (heme-reducing) electrons to be positively correlated: having opposite charges, protons and electrons will tend to stabilize each other. This is, in fact, what is observed, as shown in Fig. 6. The regions of higher correlation occur where both protonatable and redox sites are partially titrated (fully empty or occupied sites are necessarily uncorrelated). The three connected "hills" occur at the pH regions where groups of protonatable sites titrate, as already seen above for the titration surfaces and curves. The isocorrelation curves follow more or less the curves of Fig. 3, corresponding to partial reduction. The correlation surface illustrates very clearly the nonspecific nature of the redox-Bohr effect, which exists whenever protons and electrons are in binding equilibrium in the same molecule.

The analysis of the coupling between individual sites in terms of correlation surfaces like the one of Fig. 6 would require an enormous number of three-dimensional plots (one per pair of sites) and will not be presented here. Instead, we focus on the correlations of the hemes with other sites and restrict ourselves to a particular set of thermodynamic states. More exactly, we analyze only the correlations with the hemes when these are half-protonated, i.e., the correlations along the E^{half} curves of Fig. 3 *a*, which allow us to examine which sites are more strongly correlated with heme reduction. Fig. 7 shows the correlation curves with absolute values greater than 0.1; below this value there are too many correlated sites to allow for a clear analysis, so this was taken as a significance threshold. Correlations with other hemes (*dashed and dotted lines*) are negative, whereas the ones with protonatable sites (*solid lines*) are positive. As in Fig. 6, and for a more physically intuitive analysis, the correlations refer to the occupation of hemes by electrons, and not by positive charges, as in the formalism of the Theory section.

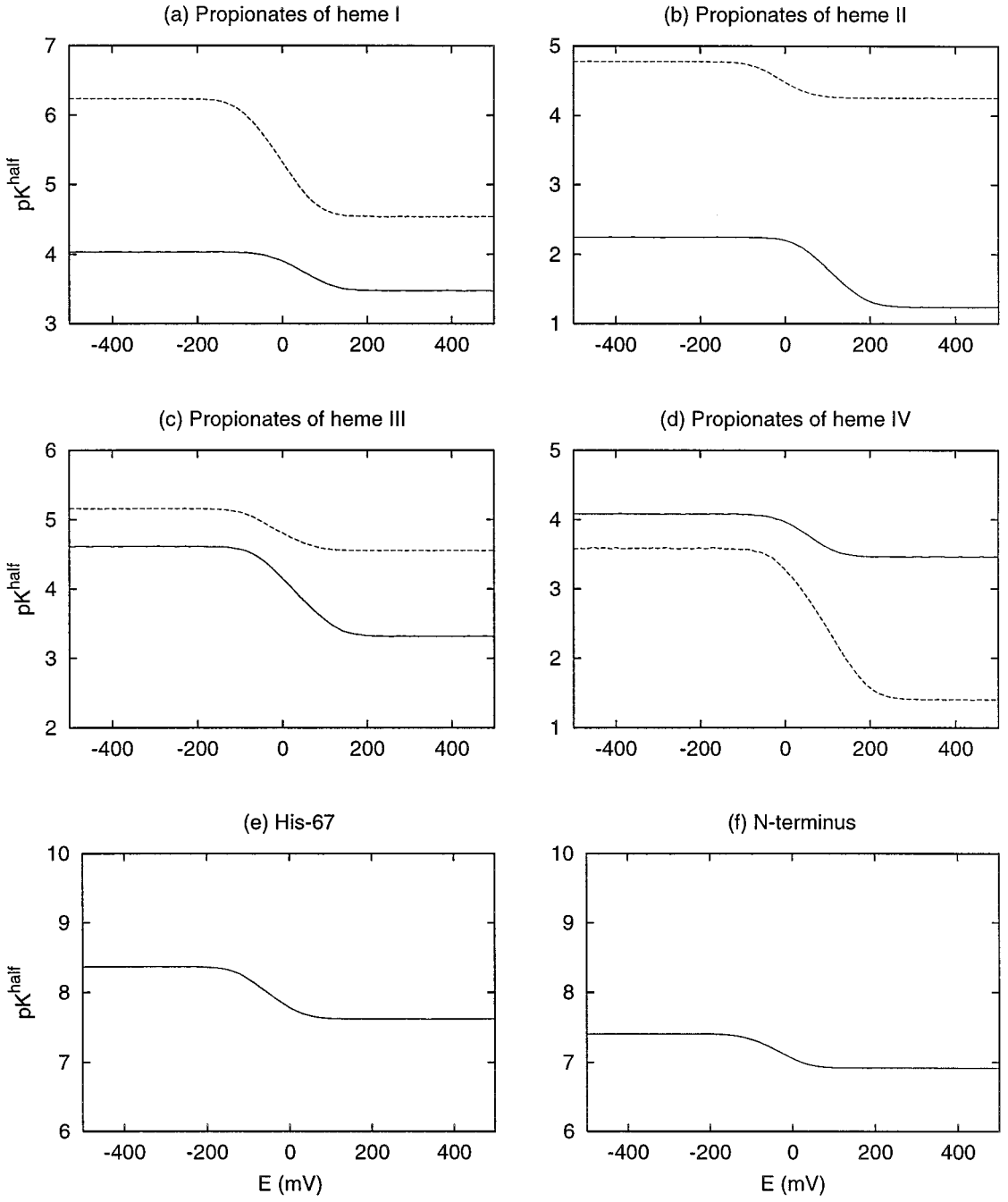

FIGURE 5 pK^{half} dependence on E for heme propionates A (*solid line*) and D (*dashed line*), and sites His^{67} and the N-terminus.

One of the more evident features in Fig. 7 is that the hemes always have large correlations with at least one of their propionate sites, which is not surprising, given their proximity. The shape of the correlation curves of the propionates D of hemes I and IV (PDI and PDIV) is particularly interesting: instead of showing a sharp peak, these sites have very broad curves with a shoulder. Although not obvious at first sight, this is also a consequence of the redox-Bohr effect, as the following reasoning shows. Significant correlations result when the half-occupation (pK^{half} or E^{half}) curves of two (directly or indirectly) interacting sites approach on the pH-E plane, the maximum correlation usually corresponding to the crossing of the two curves (not shown). This is due to the fact that when a site tends to be empty or occupied, its fluctuations are too small for the site to show any significant correlation with another one; it is simply a consequence of the definition of correlation itself. Usually, the half-occupation curves approach in a narrow region, giving rise to a relatively sharp correlation peak. However, when large pK^{half} and/or E^{half} shifts exist, the curves may stay close to each other within a much larger region of the pH-E plane, giving rise to correlation shoul-

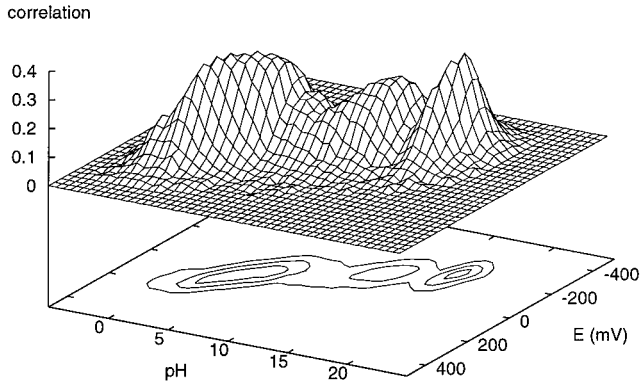

FIGURE 6 Correlation between the total number of protons and the total number of electrons, as a function of pH and *E*. The isocorrelation curves projected on the base correspond, from outer to inner ones, to 0.1, 0.2, and 0.3.

ders like the ones seen for the propionates D of hemes I and IV. Hence, the large pK^{half} shifts of these propionates, seen in Fig. 5, are due to strong interactions with the corresponding hemes.

The protonatable sites showing significant correlations in the pH region of the biological redox-Bohr effect, 5–8 (Turner et al., 1996), are His^{67}, the N-terminus, and all of the propionate sites except propionates A of hemes I and II. It is interesting that, even though the pK^{half} curves of some propionates (Fig. 5) stay below pH 5, their correlation curves extend beyond that value; one remarkable example is the propionate D of heme IV. Given that the biologically important step is probably the reduction of hemes I and II, the relevant sites in this respect are the propionates D of hemes I and II, the N-terminus, and His^{67}. This is in agreement with a previous study in which couplings were analyzed in terms of direct interactions (Soares et al., 1997), except that propionate D of heme II was not previously proposed. It is interesting that propionate D of heme I displays a significant (although weak) correlation with heme II; this may be related to the conformational change of this propionate upon reduction of heme II observed in MD simulations (Soares et al., 1998).

With regard to heme-heme couplings, significant correlations exist for pairs I–II, I–III, and III–IV, all of which correspond to hemes adjacent in the DvHc_3 molecule (only the adjacent II–IV pair is missing). The correlations between hemes are always negative, as expected in terms of direct interactions. Although positive correlations could have arisen through indirect interactions (see the three-site example above), they do not seem to be significant for heme-heme couplings in DvHc_3. Nevertheless, the correlation for the pair I–II is not particularly high, so that a conformationally induced change to positive values may be possible. The heme-heme correlations tend to stay significant over most of the pH range, because the pH-*E* titration region for the different hemes is never very different, with their E^{half} curves always staying close to each other (Fig. 3).

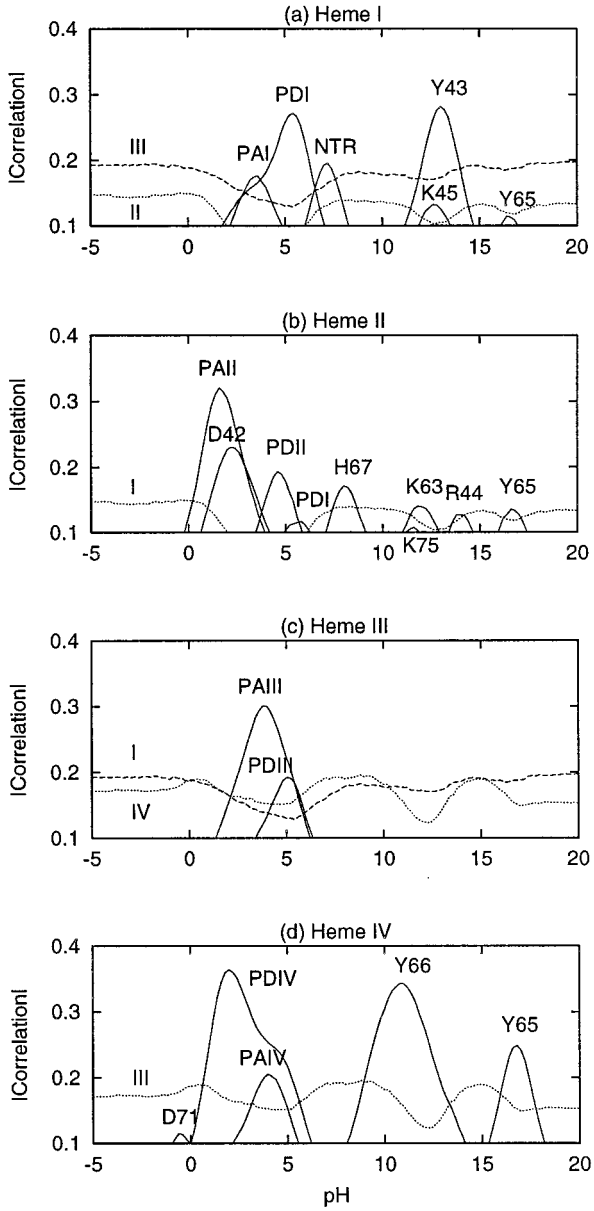

FIGURE 7 Correlations of protonatable (*solid lines*) and redox (*dashed and dotted lines*) sites with individual hemes, for the E^{half} states.

Concerted transfer and binding fluctuations

As mentioned in the Introduction, one of the proposed mechanisms in the process of H_2 cleavage by the periplasmic hydrogenase is the concerted transfer of two electrons and two protons (the products of the reactions) to cytochrome c_3 (Louro et al., 1996, 1997). Hence, at first it seems necessary that there be an excess of two net protons in cytochrome c_3 after the uptake of the two electrons. This type of analysis has been made before for DvHc_3 using CE-based pK_a calculations of particular reduction states (Soares et al., 1997), but the variation always seems to be too low to explain a concerted transfer. In Fig. 8 *a* we show those same results computed with the present methodology, using the full treatment of the protonation and redox equi-

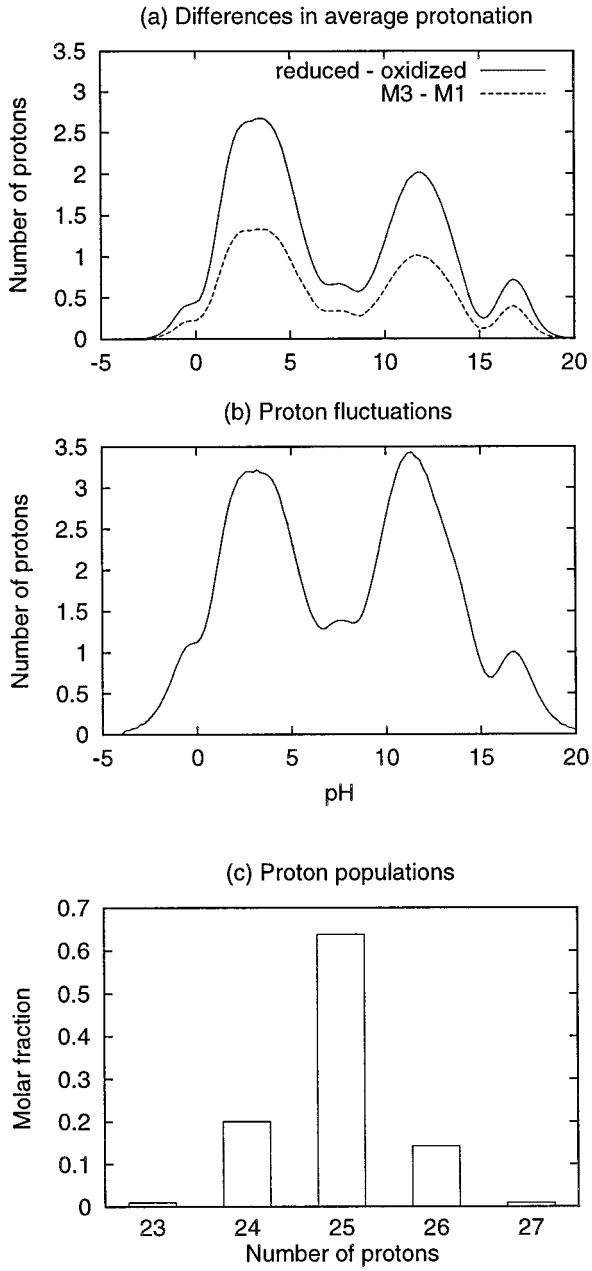

FIGURE 8 Statistics on the total number of protons. (*a*) Differences in the average values. (*b*) Fluctuations (2 SD) for state M2. (*c*) Histogram of populations for state M2 at pH 6.6.

libria. The differences are too small in the biological pH region, even if one considers the difference between the fully reduced and the fully oxidized molecule. The more realistic comparison is between the states with an average number of three and one electron, M3 and M1 (see above), whose difference is even smaller. Thus, the full equilibrium analysis of the present work does not affect significantly the previous results of net proton change and does not provide theoretical evidence for the equilibrium transfer of two protons when two electrons are captured by DvHc_3 at physiological pH.

There is, however, an alternative approach to the question of electron and proton transfer that can be made within the scope of the present equilibrium treatment, and which is based, somewhat paradoxically, on the fact that the in vivo process is probably a nonequilibrium one. Biological processes do not occur under equilibrium conditions, and organic function is only possible due to the existence of nonequilibrium fluxes of matter and energy. In particular, the processes of electron transfer are usually part of transport chains, which act as flux, nonequilibrium mechanisms. Hence, the transfer of electrons and coupled protons to and from cytochrome c_3 probably does not occur in vivo under the equilibrium conditions studied here and in most in vitro experiments, so that the conclusions of the previous paragraph do not invalidate the in vivo concerted transfer. Now, when we have detailed information on the nonequilibrium process of interest, the behavior of a system can be characterized in general by equilibrium quantities. In somewhat loose terms, the response of the system to the perturbations that keep it away from equilibrium is determined by its equilibrium fluctuations (through the fluctuation-dissipation theorem) (de Groot and Mazur, 1962; Reif, 1965; McQuarrie, 1976); this is essentially due to the fact that the perturbations cannot force the system more than it is allowed by its normal "plasticity." In the case of the electron and proton transfer in cytochrome c_3, we do not have much information on the nonequilibrium in vivo process, to say the least, so that an analysis of that type is out of question. However, we can examine how "permissive" the cytochrome is to an excess or deficit of electrons and/or protons that can, under nonequilibrium conditions, be "passed on" to or from other molecules. Hence, the protein has a "buffer" of protons and electrons that can be functionally important and may help to explain their nonequilibrium concerted transfer.

Fig. 8 *b* shows the fluctuations of the total number of protons in DvHc_3, expressed as two standard deviations (SD; ± 2 SD spans $\sim$98% of a Gaussian distribution), for state M2; almost identical plots are obtained for states M1 and M3. It is obvious that the proton fluctuations lead to higher variations in the number of protons than do the changes in redox state, in particular the change M1 $\rightarrow$ M3. This means that the protein can easily accommodate temporarily an excess of protons that can be subsequently passed to another molecule; furthermore, even if that transfer leaves it with a deficit of protons, that deficit does not excessively perturb the protein and can be maintained temporarily until new protons are received. In Fig. 8 *c* a histogram of proton populations for state M2, at physiological pH, shows that even though the molecule tends to have 25 protons, the populations with 24 and 26 protons are also stable. Hence, under these pH conditions, the protein naturally spans a range of about three protons through its binding fluctuations; if this number is added to the increase of $\sim$0.5 average protons associated with the redox change M1 $\rightarrow$ M3, the total variation is more than enough for the uptake of two protons. Obviously, these arguments do not explain the concerted electron-proton transfer in equilib-

rium conditions, where all fluctuations average out; but for nonequilibrium conditions they seem to provide a reasonable explanation of how this concerted transfer can occur despite a disagreement in terms of average quantities.

The same type of analysis can be made for the uptake of electrons. Fig. 9 *a* shows the fluctuations of the total number of electrons for states M1–M3. These fluctuations are always quite high, even though each curve corresponds to a fixed average number of electrons. Plot 9*b* shows a broad distribution of the total number of electrons, for state M2 at physiological pH. Even though the M2 state has an average number of two electrons, the molecules with two electrons are actually just one-half of the total protein population. Hence, under these pH conditions, the protein naturally spans a range of about three electrons through its binding fluctuations. This very large fluctuation may facilitate the transfer of electrons under nonequilibrium conditions, as discussed above for the case of protons, so that the uptake of two electrons may not even require the equilibrium redox change M1 → M3 assumed above.

In conclusion, electrons and protons each have a buffer of about three units that may, under appropriate nonequilibrium conditions, be totally or partially responsible for the concerted transfer of two electrons and two protons. Nevertheless, we cannot discard the possibility of equilibrium concerted transfer mediated by protonation- or reduction-mediated conformational changes (see above), which cannot be modeled by the simple CE approach used here. Furthermore, such changes may also lead to proton and electron fluctuations different from the ones computed here.

Occupational entropies

In this section we present some values for the occupational entropy contribution for binding reactions in DvHc_3, more exactly, the contributions to E^{half} and pK^{half} values. The analysis is especially important for the heme sites, because the occupational term is totally absent for the usual "static" CE-based redox calculations, which do not consider the binding equilibrium of electrons; thus, when used to compute reduction potentials, those calculations have a systematic error of the magnitude of the occupational entropy contribution.

The occupational entropy contributions to the E^{half} values of the heme sites are shown in Fig. 10. These non-null contributions arise from the change that the heme reduction induces in the binding fluctuations of sites coupled to them. Hence the variations in the plot can in general be traced back to changed interactions with particular sites. For example, the variations in $T\Delta S^{\text{occ}}$ observed for heme III above pH 10 follow the variations in its correlation with heme IV (Fig. 7 *c*); in this region heme III has no correlations with protonable sites, and its correlation with heme I is roughly constant. Thus the occupational entropy difference above pH 10 comes in this case from the change that heme III induces in the binding fluctuations of heme IV. Being due only to the fluctuations in the redox state of heme IV, this occupational entropy difference cannot be computed by using a "static" redox calculation. Another example that is easy to analyze is the peak between pH −2 and 0 seen for heme IV; this is essentially due to its interaction with Asp[71] (Fig. 7 *d*), because there are no other significant changes in its correlations within this range. In other cases the origin of the occupational entropy difference may be much more

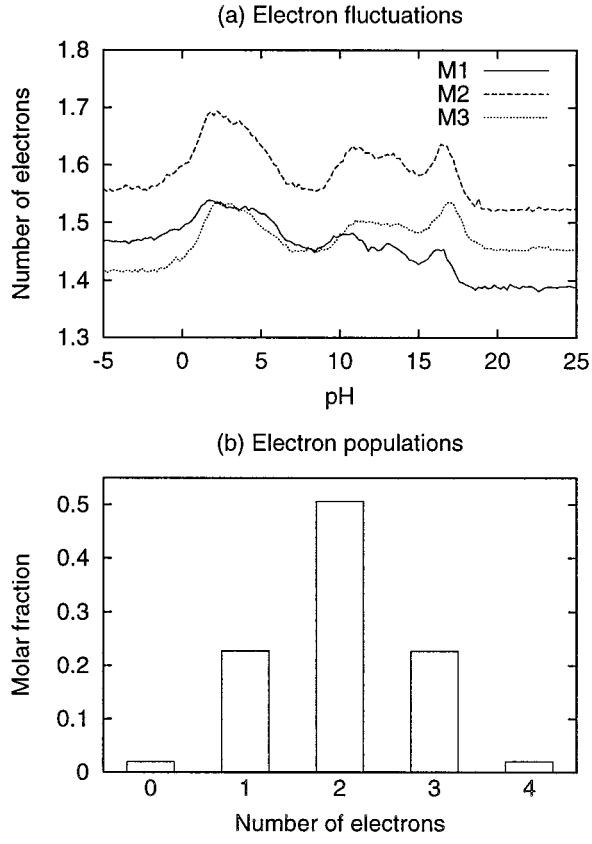

FIGURE 9 Statistics on the total number of (heme-reducing) electrons. (*a*) Fluctuations (2 SD) for states M1–M3. (*b*) Histogram of populations for state M2 at pH 6.6.

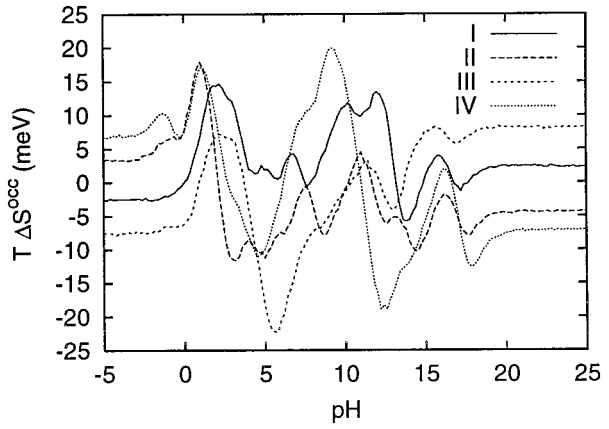

FIGURE 10 $T\Delta S^{\text{occ}}$ contributions for E^{half} values of individual hemes as a function of pH.

difficult to figure out. The important point to note is that the occupational entropy contributions to E^{half} attain values up to ± 20 meV. These are high enough to make wrong predictions of reduction order if the occupational terms are not computed (e.g., see the distances between the curves of Fig. 3 *a*).

The occupational entropy contributions to the pK^{half} values of the propionate sites, His^{67} and the N-terminus are shown in Fig. 11. The fluctuations of the occupational contributions of a protonatable site can, in principle, be traced back to individual interactions by using a correlation plot (analogous to those of Fig. 7, but for the pK^{half} state), as illustrated above for the case of redox sites; the pattern of fluctuations is actually much simpler in this case. We note that the propionates D of hemes I and IV, the more strongly interacting of these protonable sites (as seen from pK^{half} shifts and correlations), are also the ones with higher occupational entropy changes upon protonation. This is not surprising: if they are strongly coupled to other sites (including hemes), their protonation will lead to more exten-

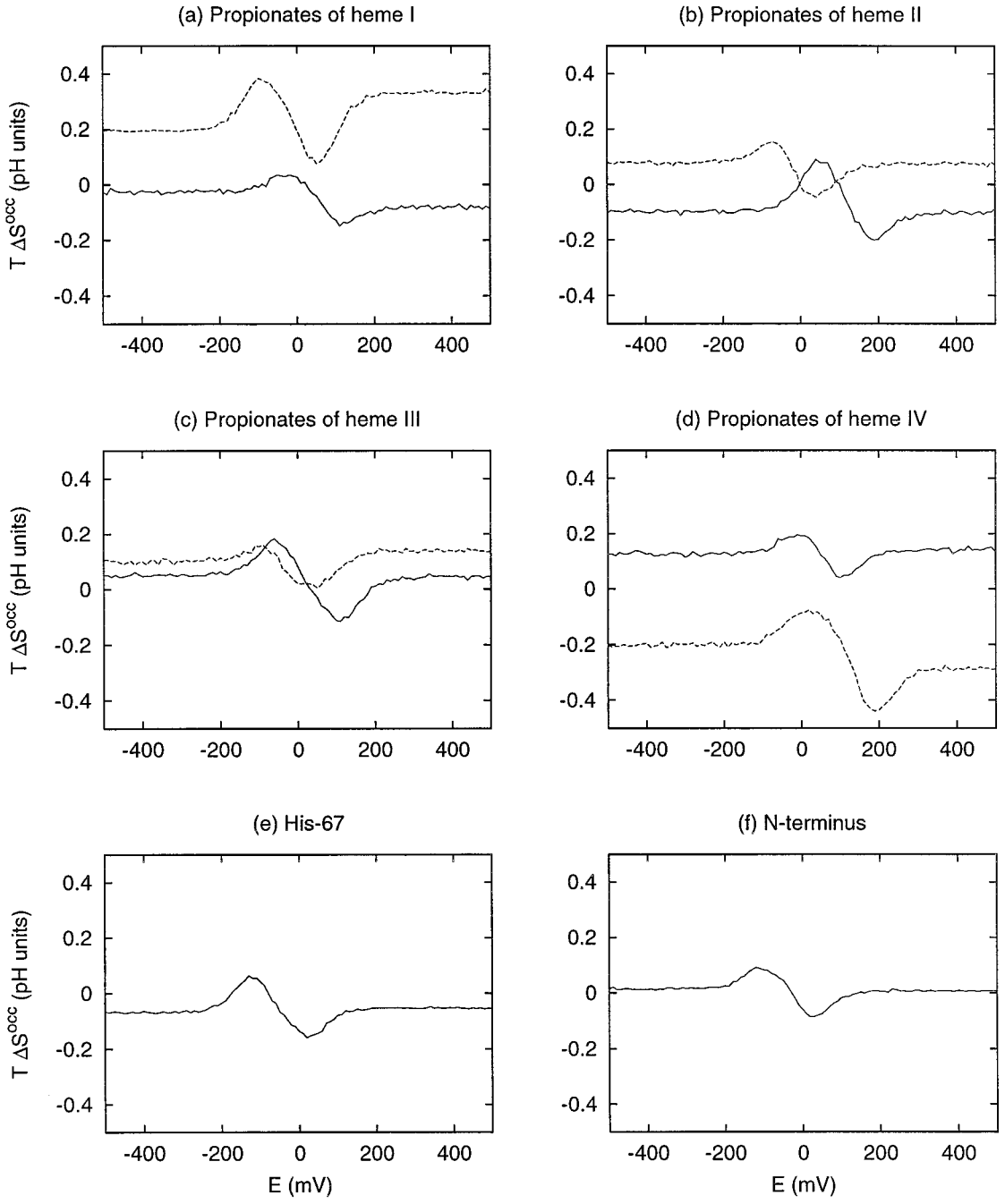

FIGURE 11 $T\Delta S^{occ}$ contributions for pK^{half} values of heme propionates A (*solid line*) and D (*dashed line*), and sites His^{67} and N-terminus, as a function of *E*.

sive changes in binding fluctuations. The occupational terms go up to ± 0.5 pH units, showing again the importance of including them by using a full equilibrium treatment of proton and electron equilibria, as done in this work.

CONCLUSIONS

This work presents a new theoretical method for treating the simultaneous binding equilibrium of electrons and protons in redox proteins, based on the use of a Monte Carlo method and CE calculations. The major advantage of this method over the usual CE-based calculations, which consider the relation between the two equilibria in a partial way (Lancaster et al., 1996; Soares et al., 1997; Kannt et al., 1998; Martel et al., 1999), is a very fundamental one: by simulating the full equilibrium of electrons and protons at a given pH and electrostatic potential of the solution, this approach tries to reproduce more faithfully the actual conditions of most in vitro and some in vivo studies. In this respect, the present "dynamic" approach is far superior to the usual "static" one. Couplings between different sites or groups of sites (e.g., electrons-protons) can be analyzed in several complementary ways, using titration surfaces and curves, pH-dependent E^{half} values, E-dependent pK^{half} values, and site-site correlations; the latter have the advantage of including the effect of indirect interactions, which are neglected by the usual comparison of interaction (free) energies. The present approach also has the advantage of including occupational entropy contributions in the computed redox potentials, which are necessarily absent from the usual "static" calculations.

The major limitation of the present approach is probably the simplified treatment of protein conformational fluctuations allowed by CE calculations, which makes impossible the occurrence of large binding-induced conformational changes. The use of the linear form of the Poisson-Boltzmann equation in the CE calculations may also lead to some inaccuracies in the electrostatic potential of surface sites. The proposed method is intended for the study of thermodynamic equilibrium (and comparisons are made with equilibrium experimental data), and, as happens with equilibrium experimental data, care must be taken in extending its conclusions to the nonequilibrium conditions typical of in vivo conditions. Nevertheless, as discussed in the Theory section, some nonequilibrium features may be inferred from the equilibrium situation.

The study of DvHc_3 by the proposed method gives a correct prediction of the reduction order of the hemes under physiological conditions; the quantitative discrepancies may be due to the existence of significant reduction-induced conformational changes in the protein (Turner et al., 1996; Soares et al., 1998), which cannot be captured within the CE approach. As for the identity of the protonatable sites more strongly involved in the biological redox-Bohr effect, the present study seems to corroborate the results of previous studies, with the propionate D of heme I being the major candidate; other sites are His^{67}, the N-terminus, and propionate D of heme IV. The possibility of concerted electron-proton transfer is shown to be unlikely in a full equilibrium situation. However, the possible role of equilibrium fluctuations in nonequilibrium transfer is discussed and proposed as an alternative explanation for the concerted transfer under in vivo nonequilibrium conditions. Finally, the occupational entropy contributions to E^{half} and pK^{half} values are shown to be significant: up to 20 mV and 0.5 pH units, respectively.

The general approach and methodology presented here can be applied to any redox protein of known structure. Obvious candidates are cytochrome *c* oxidase and the photosynthetic reaction center, already studied by the usual "static" CE approach (Gunner and Honig, 1991; Lancaster et al., 1996; Kannt et al., 1998).

APPENDIX

The standard occupational entropy change of the reaction of occupation of a site i ($n_i = 0 \rightarrow 1$) is due solely to the difference in S^{occ} between the two protein forms (with $n_i = 1$ and $n_i = 0$), because the ligands in solution only contribute to configurational entropy. The properties of these two protein forms can be treated in terms of the conditional probabilities of the global system (in a probabilistic sense a closed system is a conditional case of an open one). Hence we have

$$\begin{aligned}\Delta S_i^{\text{occ}} &= S^{\text{occ}}(n_i = 1) - S^{\text{occ}}(n_i = 0) \\ &= -k \sum_{\mathbf{n}} p(\mathbf{n}|n_i = 1)\ln p(\mathbf{n}|n_i = 1) \\ &\quad + k \sum_{\mathbf{n}} p(\mathbf{n}|n_i = 0)\ln p(\mathbf{n}|n_i = 0) \qquad \text{(A1)} \\ &= -k \sum_{\mathbf{n}} \frac{p(\mathbf{n}, n_i = 1)}{p(n_i = 1)} \ln \frac{p(\mathbf{n}, n_i = 1)}{p(n_i = 1)} \\ &\quad + k \sum_{\mathbf{n}} \frac{p(\mathbf{n}, n_i = 0)}{p(n_i = 0)} \ln \frac{p(\mathbf{n}, n_i = 0)}{p(n_i = 0)}.\end{aligned}$$

The individual probabilities can be written in terms of averages:

$$p(n_i = 1) = \langle n_i \rangle \qquad \text{(A2)}$$

$$p(n_i = 0) = 1 - \langle n_i \rangle. \qquad \text{(A3)}$$

Furthermore, the joint probabilities $p(\mathbf{n}, n_i = 1)$ and $p(\mathbf{n}, n_i = 0)$ can be replaced by $p(\mathbf{n})$ if the terms in the summations are multiplied, respectively, by n_i and $1 - n_i$. (There is no problem with vanishingly small probabilities, because

$p \ln p \to 0$ as $p \to 0$.) We then have

$$\begin{aligned}\Delta S_i^{occ} &= -\frac{k}{\langle n_i\rangle}\left[\sum_{\mathbf{n}} n_i p(\mathbf{n})\ln p(\mathbf{n}) - \ln\langle n_i\rangle \sum_{\mathbf{n}} n_i p(\mathbf{n})\right] \\ &\quad + \frac{k}{1-\langle n_i\rangle}\left[\sum_{\mathbf{n}}(1-n_i)p(\mathbf{n})\ln p(\mathbf{n})\right. \\ &\quad \left. - \ln(1-\langle n_i\rangle)\sum_{\mathbf{n}}(1-n_i)p(\mathbf{n})\right] \\ &= \frac{\langle -k\ln p(\mathbf{n}) n_i\rangle}{\langle n_i\rangle} + k\ln\langle n_i\rangle - \frac{\langle -k\ln p(\mathbf{n})(1-n_i)\rangle}{1-\langle n_i\rangle} \\ &\quad - k\ln(1-\langle n_i\rangle) \\ &= k\ln\frac{\langle n_i\rangle}{1-\langle n_i\rangle} + \frac{\langle -k\ln p(\mathbf{n}) n_i\rangle - \langle -k\ln p(\mathbf{n})\rangle\langle n_i\rangle}{\langle n_i\rangle(1-\langle n_i\rangle)}.\end{aligned} \tag{A4}$$

We now note that the numerator of the second term corresponds to the covariance between n_i and $-k \ln p(\mathbf{n})$, and the denominator to the variance of n_i (because $\langle n_i^2\rangle = \langle n_i\rangle$). By using Eq. 2 and the properties of the covariance with respect to multiplication and addition of constants, we finally obtain

$$T\Delta S_i^{occ} = kT\ln\frac{\langle n_i\rangle}{1-\langle n_i\rangle} + \frac{\mathrm{cov}[n_i,\ \Delta G(\mathbf{n}) + 2.3kT\mathbf{n}\cdot\mathbf{pL}]}{\mathrm{var}(n_i)}. \tag{A5}$$

We gratefully acknowledge Prof. Maria A. Carrondo for continuing and fruitful discussions, suggestions, and support during this work. We also thank Prof. António V. Xavier for fruitful discussions.

This work is financially supported by Junta Nacional de Investigação Científica e Tecnológica, Portugal (BPD/4151/94, PBIC/C/BIO/2037/95, BPD/9967/96, BIC/1921/97), and EC (BIO04-CT96-0413).

REFERENCES

Alden, R. G., W. W. Parson, Z. T. Chu, and A. Warshel. 1995. Calculations of electrostatic energies in photosynthetic reaction centers. *J. Am. Chem. Soc.* 117:12284–12298.

Alexov, E. G., and M. R. Gunner. 1997. Incorporating protein conformational flexibility into the calculation of pH-dependent protein properties. *Biophys. J.* 72:2075–2093.

Allen, M. P., and D. J. Tildesley. 1987. Computer Simulation of Liquids. Clarendon, Oxford.

Antosiewicz, J., J. A. McCammon, and M. K. Gilson. 1994. Prediction of pH-dependent properties of proteins. *J. Mol. Biol.* 238:415–436.

Antosiewicz, J., and D. Porschke. 1989. The nature of protein dipole moments: experimental and calculated permanent dipole of α-chymotrypsin. *Biochemistry.* 28:10072–10078.

Apostolakis, J., I. Muegge, U. Ermler, G. Fritzsch, and E. W. Knapp. 1996. Free energy computations on the shift of the special pair redox potential: mutants of the reaction center of *Rhodobacter sphaeroides. J. Am. Chem. Soc.* 118:3743–3752.

Badziong, W., and R. K. Thauer. 1978. Growth yields and growth rates of *Desulfovibrio vulgaris* (Marburg) growing on hydrogen plus sulfate and hydrogen plus thiosulfate as the sole energy source. *Arch. Microbiol.* 117:209–214.

Badziong, W., R. K. Thauer, and J. G. Zeikus. 1978. Isolation and characterization of *Desulfovibrio* growing on hydrogen plus sulfate as the sole energy source. *Arch. Microbiol.* 116:41–49.

Baptista, A. M., P. J. Martel, and S. B. Petersen. 1997. Simulation of protein conformational freedom as a function of pH: constant-pH molecular dynamics using implicit titration. *Proteins.* 27:523–544.

Bashford, D., D. A. Case, C. Dalvit, L. Tennant, and P. E. Wright. 1993. Electrostatic calculations of side-chain pK_a values in myoglobin and comparison with NMR data for histidines. *Biochemistry.* 32:8045–8056.

Bashford, D., and K. Gerwert. 1992. Electrostatic calculations of the pK_a values of ionizable groups in bacteriorhodopsin. *J. Mol. Biol.* 224: 473–486.

Bashford, D., and M. Karplus. 1990. pK_a's of ionizable groups in proteins: atomic detail from a continuum electrostatic model. *Biochemistry.* 29: 10219–10225.

Bashford, D., M. Karplus, and G. W. Canters. 1988. Electrostatic effects of charge perturbations introduced by metal oxidation in proteins. *J. Mol. Biol.* 203:507–510.

Ben-Naim, A. 1992. Statistical Thermodynamics for Chemists and Biochemists. Plenum Press, New York.

Beroza, P., D. R. Fredkin, M. Y. Okamura, and G. Feher. 1991. Protonation of interacting residues in a protein by a Monte Carlo method: application to lysozyme and the photosynthetic reaction center of *Rhodobacter sphaeroides. Proc. Natl. Acad. Sci. USA.* 88:5804–5808.

Bertrand, P., O. Mbarki, M. Asso, L. Blanchard, F. Guerlesquin, and M. Tegoni. 1995. Control of the redox potential in *c*-type cytochromes: importance of the entropic contribution. *Biochemistry.* 34:11071–11079.

Beveridge, D. L., and F. M. DiCapua. 1989. Free energy via molecular simulation: application to chemical and biomolecular systems. *Annu. Rev. Biophys. Biophys. Chem.* 18:431–492.

Churg, A. K., and A. Warshel. 1986. Control of the redox potential of cytochrome *c* and microscopic dielectric effects in proteins. *Biochemistry.* 25:1675–1681.

Coletta, M., T. Catarino, J. LeGall, and A. V. Xavier. 1991. A thermodynamic model for the cooperative functional properties of the tetraheme cytochrome c_3 from *Desulfovibrio gigas. Eur. J. Biochem.* 202: 1101–1106.

Cutler, R. L., A. M. Davies, S. Creighton, A. Warshel, G. R. Moore, M. Smith, and A. G. Mauk. 1989. Role of arginine-38 in regulation of the cytochrome *c* oxidation-reduction equilibrium. *Biochemistry.* 28: 3188–3197.

Czjzek, M., F. Payan, F. Guerlesquin, M. Bruschi, and R. Haser. 1994. Crystal structure of cytochrome c_3 from *Desulfovibrio desulfuricans* Norway at 1.7 Å resolution. *J. Mol. Biol.* 243:653–667.

de Groot, S. R., and P. Mazur. 1962. Non-Equilibrium Thermodynamics. North-Holland, Amsterdam.

Del Buono, G. S., F. E. Figueirido, and R. M. Levy. 1994. Intrinsic pK_as of ionizable residues in proteins: an explicit solvent calculation for lysozyme. *Proteins.* 20:85–97.

Demchuk, E., and R. C. Wade. 1996. Improving the continuum dielectric approach to calculating pK_as of ionizable groups in proteins. *J. Phys. Chem.* 100:17373–17387.

Gilson, M. K., and B. H. Honig. 1986. The dielectric constant of a folded protein. *Biopolymers.* 25:2097–2119.

Gilson, M. K., and B. Honig. 1988. Energetics of charge-charge interactions in proteins. *Proteins.* 3:32–52.

Gilson, M. K., K. A. Sharp, and B. Honig. 1987. Calculating the electrostatic potential of proteins in solution: method and error assessment. *J. Comput. Chem.* 9:327–335.

Gunner, M. R., and B. Honig. 1991. Electrostatic control of midpoint potentials in the cytochrome subunit of the *Rhodopseudomonas viridis* reaction center. *Proc. Natl. Acad. Sci. USA.* 88:9151–9155.

Harbury, H. A., J. R. Cronin, M. W. Fanger, T. P. Hettinger, A. J. Murphy, Y. P. Myer, and S. N. Vinogradov. 1965. Complex formation between methionine and a heme peptide from cytochrome *c. Proc. Natl. Acad. Sci. USA.* 54:1658–1664.

Hastings, W. K. 1970. Monte Carlo sampling methods using Markov chains and their applications. *Biometrika.* 57:97–109.

Higuchi, Y., M. Kusunoki, Y. Matsuura, N. Yasuoka, and M. Kakudo. 1984. Refined structure of cytochrome c_3 at 1.8 Å resolution. *J. Mol. Biol.* 172:109–139.

Hill, T. L. 1960. An Introduction to Statistical Thermodynamics. Addison-Wesley, Reading, MA.

Honig, B., and A. Nicholls. 1995. Classical electrostatics in biology and chemistry. *Science.* 268:1144–1149.

Hooft, R. W. W., C. Sander, and G. Vriend. 1996. Positioning hydrogen atoms by optimizing hydrogen-bond networks in protein structures. *Proteins.* 26:363–376.

Kannt, A., C. R. D. Lancaster, and H. Michel. 1998. The coupling of electron transfer and proton translocation: electrostatic calculations on *Paracocus denitrificans* cytochrome *c* oxidase. *Biophys. J.* 74:708–721.

Lancaster, C. R. D., H. Michel, B. Honig, and M. R. Gunner. 1996. Calculated coupling of electron and proton transfer in the photosynthetic reaction center of *Rhodopseudomonas viridis*. *Biophys. J.* 70: 2469–2492.

Langen, R., G. M. Jensen, U. Jacob, P. J. Stephens, and A. Warshel. 1992. Protein control of iron-sulfur cluster redox potentials. *J. Biol. Chem.* 267:25625–25627.

Lee, F. S., Z. T. Chu, and A. Warshel. 1993. Microscopic and semimicroscopic calculations of electrostatic energies in proteins by the POLARIS and ENZYMIX programs. *J. Comput. Chem.* 14:161–185.

Levy, R. M., M. Belhadj, and D. B. Kitchen. 1991. Gaussian fluctuation formula for electrostatic free-energy changes in solution. *J. Chem. Phys.* 95:3627–3633.

Louro, R. O., T. Catarino, J. LeGall, and A. V. Xavier. 1997. Redox-Bohr effect in electron/proton energy transduction: cytochrome c_3 coupled to hydrogenase works as a "proton thruster" in *Desulfovibrio vulgaris. J. Biol. Inorg. Chem.* 2:488–491.

Louro, R. O., T. Catarino, C. A. Salgueiro, J. LeGall, and A. V. Xavier. 1996. Redox-Bohr effect in the tetrahaem cytochrome c_3 from *Desulfovibrio vulgaris*: a model for energy transduction mechanism. *J. Biol. Inorg. Chem.* 1:34–38.

Mark, A. E., and W. F. van Gunsteren. 1994. Decomposition of the free energy of a system in terms of specific interactions. *J. Mol. Biol.* 240:167–176.

Martel, P. J., C. M. Soares, A. M. Baptista, M. Fuxreiter, G. Náray-Szabó, and M. A. Carrondo. 1999. Comparative redox and pK_a calculations on cytochrome c_3 from several *Desulfovibrio* species using continuum electrostatic methods. *J. Biol. Inorg. Chem.* (in press).

Matias, P. M., C. Frazão, J. Morais, M. Coll, and M. A. Carrondo. 1993. Structure analysis of cytochrome c_3 from *Desulfovibrio vulgaris* Hildenborough at 1.9 Å resolution. *J. Mol. Biol.* 234:680–699.

Matias, P. M., J. Morais, R. Coelho, M. A. Carrondo, K. Wilson, Z. Dauter, and L. Sieker. 1996. Cytochrome c_3 from *Desulfovibrio gigas*: crystal structure at 1.8 Å resolution and evidence for a specific calcium-binding site. *Protein Sci.* 5:1342–1354.

McQuarrie, D. A. 1976. Statistical Mechanics. Harper, New York.

Messias, A. C., D. H. W. Kastrau, H. S. Costa, J. LeGall, D. L. Turner, H. Santos, and A. V. Xavier. 1998. Solution structure of *Desulfovibrio vulgaris* (Hildenborough) ferrocytochrome c_3: structural basis for functional cooperativity. *J. Mol. Biol.* 281:719–739.

Metropolis, N., A. W. Rosenbluth, M. N. Rosenbluth, A. H. Teller, and E. Teller. 1953. Equation of state calculations by fast computing machines. *J. Chem. Phys.* 21:1087–1092.

Mezei, M., and D. L. Beveridge. 1986. Free energy simulations. *Ann. N.Y. Acad. Sci.* 482:1–23.

Mood, A. M., F. A. Graybill, and D. C. Boes. 1974. Introduction to the Theory of Statistics, 3rd Ed. McGraw-Hill, New York.

Morais, J., P. N. Palma, C. Frazão, J. Caldeira, J. LeGall, I. Moura, J. J. Moura, and M. A. Carrondo. 1995. Structure of the tetraheme cytochrome from *Desulfovibrio desulfuricans* ATCC 27774: x-ray diffraction and electron paramagnetic resonance studies. *Biochemistry.* 34: 12830–12841.

Muegge, I., P. X. Qi, A. J. Wand, Z. T. Chu, and A. Warshel. 1997. The reorganization energy of cytochrome *c* revisited. *J. Chem. Phys. B.* 101:825–836.

Nozaki, Y., and C. Tanford. 1967. Examination of titration behavior. *Methods Enzymol.* 11:715–734.

Papa, S., F. Guerrieri, and G. Izzo. 1979. Redox Bohr-effects in the cytochrome system in mitochondria. *FEBS Lett.* 105:213–216.

Park, J.-S., T. Ohmura, K. Kano, T. Sagara, K. Niki, Y. Kyogoku, and H. Akutsu. 1996. Regulation of the redox order of four hemes by pH in cytochrome c_3 from *D. vulgaris* Miyazaki F. *Biochim. Biophys. Acta.* 1293:45–54.

Reif, F. 1965. Fundamentals of Statistical and Thermal Physics. McGraw-Hill, New York.

Russell, S. T., and A. Warshel. 1985. Calculations of electrostatic energies in proteins. The energetics of ionized groups in bovine pancreatic trypsin inhibitor. *J. Mol. Biol.* 185:389–404.

Salgueiro, C. A., D. L. Turner, J. LeGall, and A. V. Xavier. 1997. Reevaluation of the redox and redox-Bohr cooperativity in tetrahaem *Desulfovibrio vulgaris* (Miyazaki F) cytochrome c_3. *J. Biol. Inorg. Chem.* 2:343–349.

Salgueiro, C. A., D. L. Turner, H. Santos, J. LeGall, and A. V. Xavier. 1994. Assignment of the redox potentials to the four haems in *Desulfovibrio vulgaris* cytochrome c_3 by 2D-NMR. *FEBS Lett.* 314:155–158.

Santos, H., J. J. G. Moura, I. Moura, J. LeGall, and A. V. Xavier. 1984. NMR studies of electron transfer mechanisms in a protein with interacting redox centres: *Desulfovibrio gigas* cytochrome c_3. *Eur. J. Biochem.* 141:283–296.

Saraiva, L. M., C. A. Salgueiro, P. N. da Costa, A. C. Messias, J. LeGall, W. M. A. M. van Dongen, and A. V. Xavier. 1998. Replacement of lysine 45 by uncharged residues modulates the redox-Bohr effect in tetraheme cytochrome c_3 of *Desulfovibrio vulgaris* (Hildenborough). *Biochemistry.* 37:12160–12165.

Schellman, J. A. 1975. Macromolecular binding. *Biopolymers.* 14: 999–1018.

Sharp, K. A., and B. Honig. 1990. Electrostatic interactions in macromolecules: theory and applications. *Annu. Rev. Biophys. Biophys. Chem.* 19:301–332.

Smith, L. J., A. E. Mark, C. M. Dobson, and W. F. van Gunsteren. 1995. Comparison of MD simulations and NMR experiments for hen lysozyme: analysis of local fluctuations, cooperative motions and global changes. *Biochemistry.* 34:10918–10931.

Soares, C. M., P. J. Martel, and M. A. Carrondo. 1997. Theoretical studies of the redox-Bohr effect in cytochrome c_3 from *Desulfovibrio vulgaris* Hildenborough. *J. Biol. Inorg. Chem.* 2:714–727.

Soares, C. M., P. J. Martel, J. Mendes, and M. A. Carrondo. 1998. Molecular dynamics simulation of cytochrome c_3: studying the reduction processes using free energy calculations. *Biophys. J.* 74:1708–1721.

Tanford, C., and J. G. Kirkwood. 1957. Theory of protein titration curves. I. General equations for impenetrable spheres. *J. Am. Chem. Soc.* 79: 5333–5339.

Turner, D. L., C. A. Salgueiro, T. Catarino, J. LeGall, and A. V. Xavier. 1994. Homotropic and heterotropic cooperativity in the tetrahaem cytochrome c_3 from *Desulfovibrio vulgaris. Biochim. Biophys. Acta.* 1187: 232–235.

Turner, D. L., C. A. Salgueiro, T. Catarino, J. LeGall, and A. V. Xavier. 1996. NMR studies of cooperativity in the tetrahaem cytochrome c_3 from *Desulfovibrio vulgaris. Eur. J. Biochem.* 241:723–731.

van Gunsteren, W. F., and H. J. C. Berendsen. 1987. Groningen Molecular Simulation (GROMOS) Library Manual. Biomos, Groningen, the Netherlands.

Vorobjev, Y. N., H. A. Scheraga, B. Hitz, and B. Honig. 1994. Theoretical modeling of electrostatic effects of titrable side-chain groups on protein conformation in a polar ionic solution. 1. Potential of mean force between charged lysine residues and titration of poly(L-lysine) in 95% methanol solution. *J. Phys. Chem.* 98:10940–10948.

Vriend, G. 1990. WHAT IF: a molecular modeling and drug design program. *J. Mol. Graph.* 8:52–56.

Warshel, A. 1981. Calculations of enzymatic reactions: calculations of pK_a, proton transfer reactions, and general acid catalysis reactions in enzymes. *Biochemistry.* 20:3167–3177.

Warshel, A., and J. Åqvist. 1991. Electrostatic energy and macromolecular function. *Annu. Rev. Biophys. Biophys. Chem.* 20:267–298.

Warshel, A., and A. Papazyan. 1998. Electrostatic effects in macromolecules: fundamental concepts and practical modeling. *Curr. Opin. Struct. Biol.* 8:211–217.

Warshel, A., and S. T. Russell. 1984. Calculations of electrostatic interactions in biological systems and in solutions. *Q. Rev. Biophys.* 17: 283–422.

Warshel, A., F. Sussman, and G. King. 1986. Free energy of charges in solvated proteins: microscopic calculations using a reversible charging process. *Biochemistry.* 25:8368–8372.

Weast, R. C., editor. 1984. Handbook of Chemistry and Physics. CRC Press, Boca Raton, FL.

Wyman, J., Jr. 1964. Linked functions and reciprocal effects in hemoglobin: a second look. *Adv. Protein Chem.* 19:223–286.

Xavier, A. V. 1985. *In* Frontiers in Bioinorganic Chemistry. A. V. Xavier, editor. VCH Publishers, Weinheim, Germany. 722–725.

Yang, A.-S., M. R. Gunner, R. Sampogna, K. Sharp, and B. Honig. 1993. On the calculation of pK_a's in proteins. *Proteins.* 15:252–265.

Zwanzig, R. W. 1954. High-temperature equation of state by a perturbation method. I. Nonpolar gases. *J. Chem. Phys.* 22:1420–1426.